

NMR studies of lignin and lignin-derived products: recent advances and perspectives

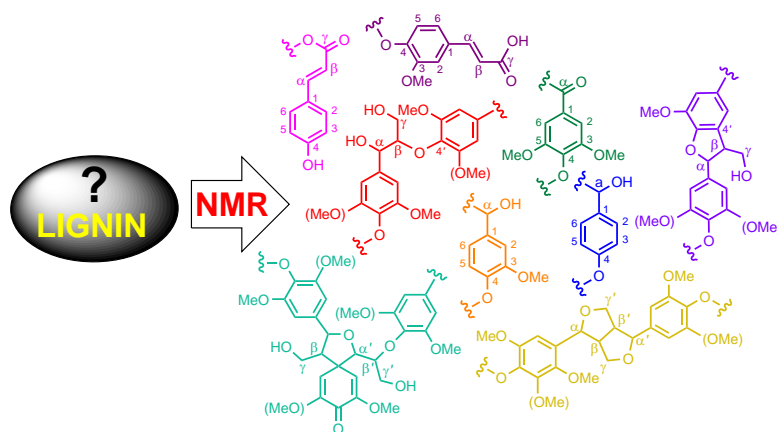
Leonid B. Krivdin 

A.E.Favorsky Irkutsk Institute of Chemistry, Siberian Branch of the Russian Academy of Sciences, 664033 Irkutsk, Russia

The present review focuses on the most recent results of a liquid-phase nuclear magnetic resonance (NMR) study of lignin together with the lignin-derived products and related chemicals. Collected and discussed are the recent applications of ^1H , ^{13}C and ^{31}P NMR spectroscopy as well as the NMR of less popular nuclei to the structural studies and practical recommendations in this field. Due to the complexity of lignin and the products of its transformation, their NMR spectra consist of a number of overlapping signals belonging to different structural types. In this regard, comprehensive studies of lignin by NMR over the past few decades have revealed characteristic functional groups of lignin and lignin-related products together with the spectral regions in which they resonate. Quantitative NMR spectra of ^1H , ^{13}C together and less popular nuclei such as ^{31}P are used to characterize different structural units of lignin (such as guaiacyl, syringyl and *p*-hydroxyphenyl), which provide aromatic and saturated carbons spread over many structural moieties.

The bibliography includes 54 references.

Keywords: liquid-phase NMR, lignin, lignin structure, lignin processing.



Contents

1. Introduction	1	2.3. ^{31}P NMR	16
2. Most recent NMR studies of lignin and lignin-derived products	3	2.4. NMR of other nuclei	19
2.1. ^1H and ^{13}C one-dimensional NMR	3	3. Conclusion	20
2.2. ^1H and ^{13}C two-dimensional NMR	7	4. List of abbreviations	25
		5. References	26

1. Introduction

Lignin is a prospective biomass-derived source for the production of some crucial organic building blocks, typically derived from unsustainable and non-renewable petroleum feedstocks.¹ Lignin, a source of plant-based biomass, is a complex cross-linked phenolic polymer, as shown in Figure 1.² As a complex polymer, lignin characterization is often challenging due to its random structure and multitudes of different repeating molecular substructures.

Identified structural units of lignin are shown in Figure 1 and characteristic heteronuclear single quantum coherence (HSQC) NMR spectrum of spruce milled wood lignin is presented in Figure 2. Aromatic structures present in lignin are as follows: syringyl unit, oxidized syringyl unit, guaiacyl unit,

p-hydroxyphenyl unit, ferulic acid, cinnamyl alcohol end group, cinnamaldehyde end group, and *p*-coumaric acid, while the main linkages of lignin are β -aryl-ether β -O-4, resinol β - β , phenylcoumaran β -5 and spirodienone.

This polymer is crucial to the structural integrity of cell walls in wood and bark and has been extensively studied. As a by-product of paper production, lignin is used for fast energy generation. However, lignin proved to be an exceptional source of organic building blocks, many of which are currently obtained from petroleum feedstocks. Lignin, a natural biopolymer and an abundant by-product, is a particularly promising feedstock for carbon-based materials and a potentially sustainable alternative to phenolic resins, which are typically derived from crude oil. Among different types of biomass, lignin is the most abundant aromatic biopolymer and a potential source for industrial products.

The structure of lignin is highly dependent on its origin. While softwood lignins contain mainly guaiacyl units with negligible amounts of *p*-hydroxyphenyl groups, hardwood lignins are composed of guaiacyl and syringyl subunits. Grass lignins are constituted by guaiacyl (**G**), syringyl (**S**), and *p*-hydroxyphenyl (**H**) subunits.

L.B.Krivdin. DSc (Chemistry), Professor, Chief Researcher at the Laboratory of Nuclear Magnetic Resonance of the Irkutsk Institute of Chemistry, Siberian Branch of the Russian Academy of Sciences. E-mail: krivdin55@gmail.com

Current research interests: NMR spectroscopy, quantum-chemical calculations, natural products, fuel feedstock.

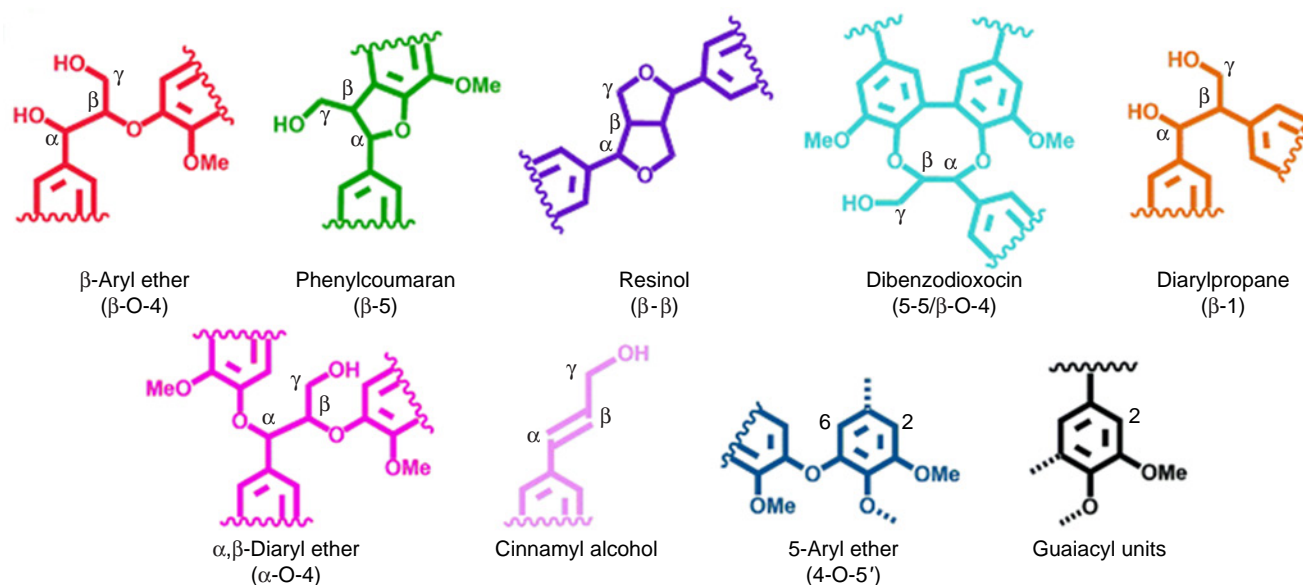


Figure 1. Identified structural units of lignin. Reproduced from Balakshin *et al.*² under the Attribution-NonCommercial 4.0 International Public License (CC BY-NC 4.0).

In general, NMR provides direct information on lignin structure and its chemical composition. In particular, data from quantitative monodimensional ^1H and ^{13}C NMR spectra together with heteronuclear and multidimensional NMR data provide information on different types of lignin interunit bondings.³ Unfortunately, monodimensional spectra suffer from significant signal overlap, which seriously hampers signal integration. Quantitative HSQC has been used to understand lignin framework, providing direct information on internal linkages and also giving general insights into

lignin structure based on the early ^1H and ^{13}C NMR (see Refs 4–9) together with ^{31}P NMR (see Ref. 10) data on modified lignin.

However, although a part of the lignin chemistry community has used HSQC as a quantitative or semi-quantitative tool in recent years, this is not scientifically rigorous and therefore, acceptable due to the intrinsic nature of the pulse sequence. Quantitative ^1H – ^{13}C HSQC measurements have recently greatly facilitated lignin analyses. In some cases, however, long acquisition times

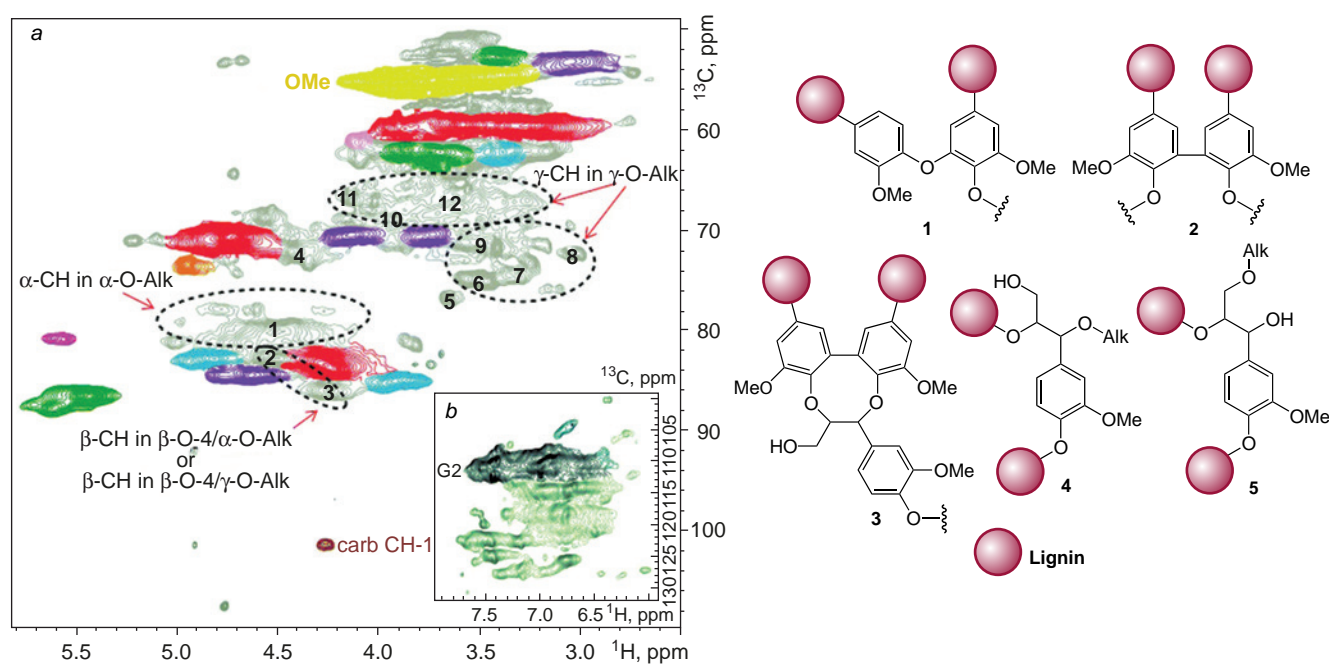


Figure 2. Different lignin branching/cross-linking units: (1) etherified 4-O-5', (2) etherified 5-5', (3) dibenzodioxocin (DBDO), (4) α -O-Alk/ β -O-4, and (5) γ -O-Alk/ β -O-4. Given in the lower part is the HSQC NMR spectrum of spruce milled wood lignin in $\text{DMSO}-d_6$: (a) side-chain region; (b) aromatic region. Reproduced from Balakshin *et al.*² under the Attribution-NonCommercial 4.0 International Public License (CC BY-NC 4.0).

were needed for obtaining quantitative HSQC, which are incompatible with the chemical integrity of the (potentially functionalized) lignin sample.

Sette *et al.*⁹ compared different methods that were developed for the more time-efficient quantitative HSQC measurements with respect to their usefulness in lignin analysis. As a result, reliable and reproducible results were obtained using both the QQ-HSQC and HSQC₀ methods. Indeed, an obstacle to the development of a reliable relationship between lignin structure and upgradeability is the difficulty to quantitatively measure lignin structural features by means of classical HSQC. Amiri *et al.*¹¹ demonstrated that a modified HSQC method known as HSQC₀, can accurately quantify lignin functionalities in extracted lignin. In 2024, Bourmaud *et al.*¹² developed a rapid elevated-temperature ¹H–¹³C heteronuclear single-quantum coherence zero (HSQC₀) method that enables a precise quantification of the kraft lignin structural characteristics even with whole plant cell wall (known as ‘HSQC₀ WPCW’). Such analysis illustrates how this analytical method can greatly facilitate the study of kraft lignin structure, which can then be used for the fundamental studies of lignin.

Recent applications of ¹H, ¹³C, and ³¹P NMR spectroscopy together with NMR of less popular nuclei like ³¹P, ¹⁹F, and ¹⁵N to the structural studies of lignin provide a breakthrough and practical guide in this field. The structural NMR studies of lignin are developing on a backdrop of a marked progress in computational NMR of hydrogen^{13–15} and carbon,^{16–20} the elements which are the main constituents of lignin, together with NMR of phosphorous,^{21,22} provided lignin is labelled with ³¹P isotope to offer lignin analysis by means of ³¹P NMR.

2. Most recent NMR studies of lignin and lignin-derived products

2.1. ¹H and ¹³C one-dimensional NMR

A representative example of NMR studies of lignin carried out in the last five years is the paper by Levdansky *et al.*,²³ which deals with the NMR study of the soluble organosolv lignins extracted from fir and aspen wood. Fir and aspen lignins were found to be of the **G** and **GS** types, respectively. The one-dimensional ¹H and ¹³C NMR spectra of these samples are illustrated in Figures 3 and 4, respectively. The authors also found that the β-O-4' linkages in ethanol lignins extracted from

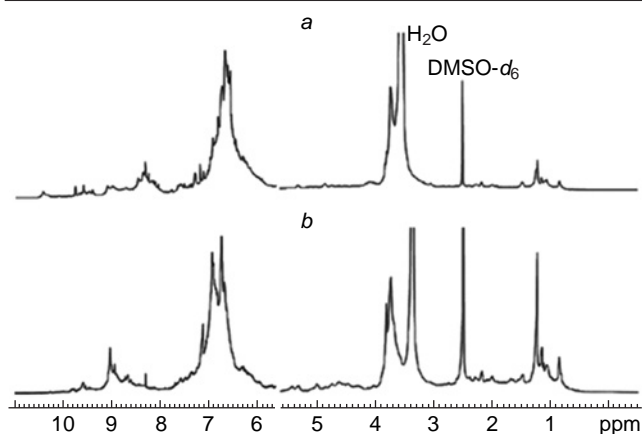


Figure 3. ¹H NMR spectra of ethanol lignins extracted from aspen (a) and fir (b). All ¹H NMR spectra were recorded on a Bruker Avance 600 NMR spectrometer operating at 600 MHz in DMSO-*d*₆. Reproduced with minor editing privileges from Levdansky *et al.*²³ with the permission of the Siberian Federal University.

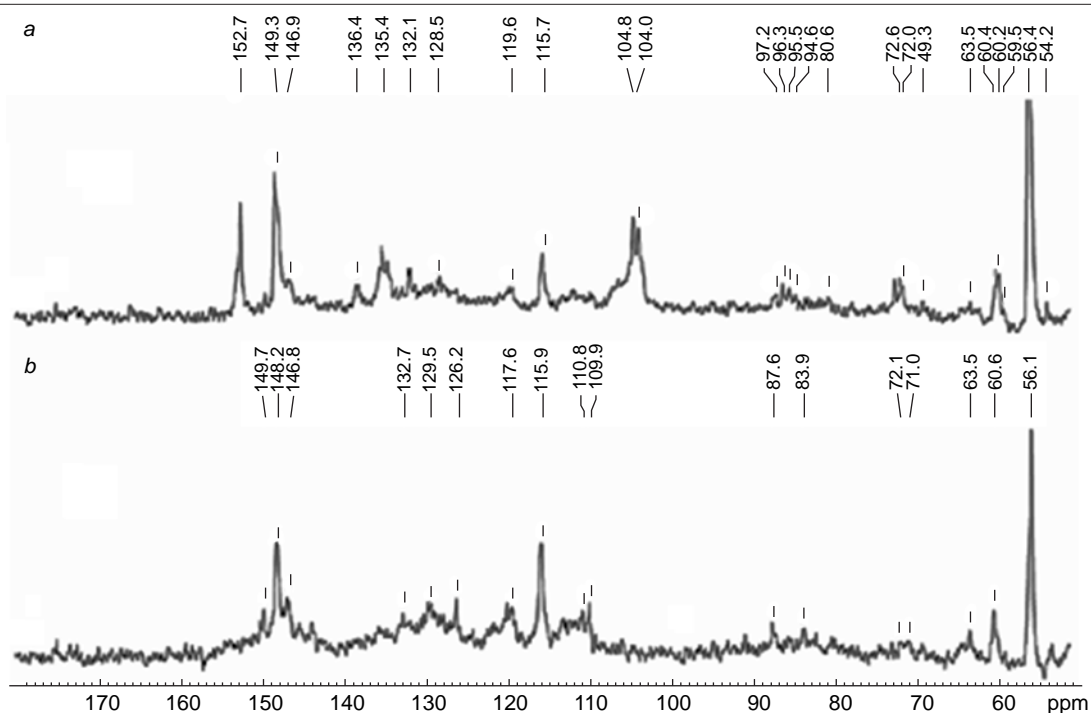


Figure 4. ¹³C NMR spectra of ethanol lignins extracted from aspen (a) and fir (b). All ¹³C NMR spectra were recorded on a Bruker Avance 600 NMR spectrometer operating at 150 MHz in DMSO-*d*₆. Reproduced with minor editing privileges from Levdansky *et al.*²³ with the permission of the Siberian Federal University.

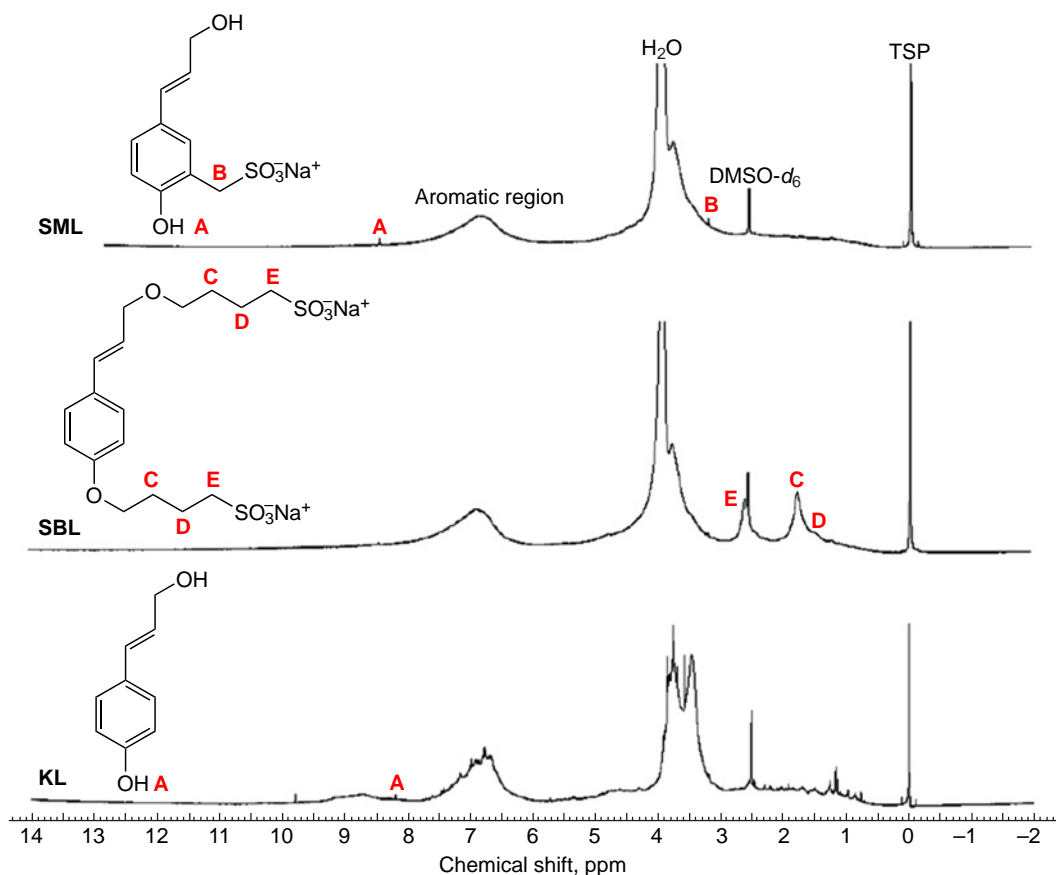


Figure 5. ^1H NMR spectra of kraft lignin (KL), sulfomethylated lignin (SML), and sulfobutylated lignin (SBL) recorded on the INOVA-500 NMR spectrometer (Varian) operating at 500 MHz in DMSO-*d*₆. TSP = Me₃Si(CH₂)₂CO₂H. Reproduced from Hopa and Fatehi²⁴ under the Attribution-NonCommercial 4.0 International Public License (CC BY-NC 4.0).

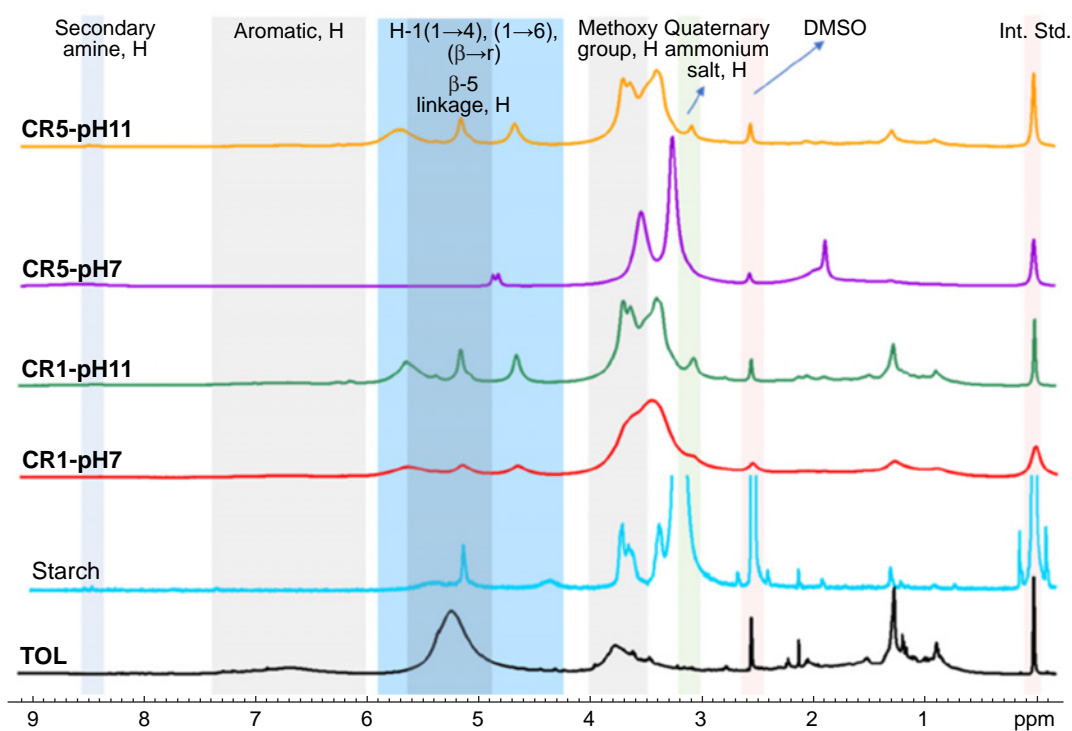


Figure 6. ^1H NMR spectra of cationic TOL-starch copolymers, starch and TOL recorded on the AVANCE NEO-1.2 GHz spectrometer (Bruker, USA) operating at 1.2 GHz in DMSO-*d*₆. Int. Std. is internal standard. Reproduced from Zhao *et al.*²⁵ with the permission of Elsevier.

fir and aspen were partially ethoxylated and contained the ethoxy groups in the α -position.

Hopa and Fatehi²⁴ studied sulfoalkylated lignin derivatives obtained by sulfomethylation and sulfobutylation of kraft lignin. The ^1H NMR spectra of kraft lignin and its sulfomethylated and sulfobutylylated derivatives, shown in Figure 5, were used to identify those structures. In the spectrum of kraft lignin, two broad peaks at 6.8–7.5 and 3.2–3.8 ppm were attributed to the protons of aromatic ring and methoxy groups, respectively. In the spectrum of sulfomethylated lignin, these peaks were found to be much weaker than those of kraft lignin due to the cleavage of aromatic ring and methoxy groups during sulfomethylation. The peak at 8.2 ppm (assigned by the authors to proton **A**) represented the hydrogen of the phenolic hydroxyls. In the spectrum of sulfomethylated lignin, the peak at 3.23 ppm (assigned to proton **B**) was attributed to the signal of the methylene groups. In the spectrum of sulfobutylylated lignin, three peaks at 1.79, 1.58, and 2.63 ppm were assigned to **C**, **D**, and **E** protons, respectively, which were absent in the spectrum of the starting kraft lignin.

In 2023, Zhao *et al.*²⁵ prepared a novel cationic tall oil lignin (**TOL**)-starch copolymer by the polymerization of **TOL**, starch and a cationic monomer of (3-acrylamidopropyl) trimethyl ammonium chloride (APTAC) through the free radical chain extension. Based on the ^1H NMR and ^1H – ^1H Correlated Spectroscopy (COSY) experiments, it was found that **TOL** and starch were covalently linked by the APTAC to produce corresponding cationic copolymers. One-dimensional and ^1H – ^1H COSY spectra of the cationic copolymers prepared with a ratio of APTAC to **TOL** of 1 or 5 in the neutral or basic reaction medium (designated as CR1-pH7, CR1-pH11, CR5-pH7, and CR5-pH11, respectively) together with the pristine starch and **TOL** are shown in Figures 6 and 7 as examples. For the origin and numbering of the fractions, see the original publication. In general, it was shown that the structure of cationic copolymers comprised anhydroglucose unit of starch, the phenolic structure

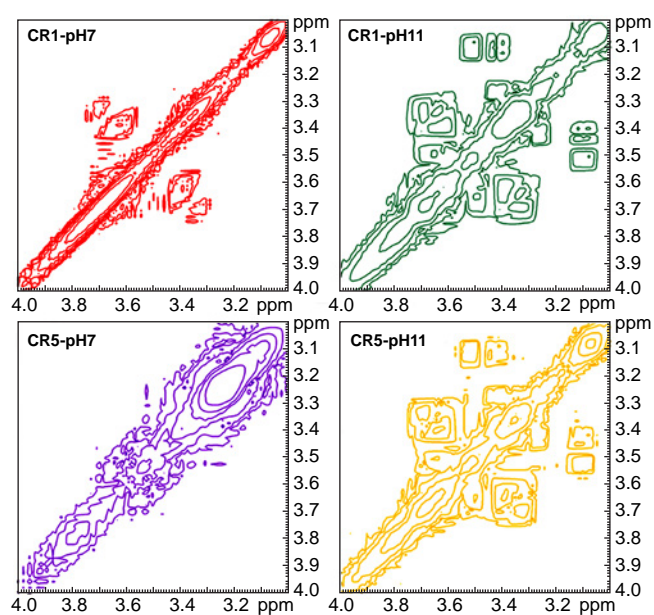


Figure 7. 2D ^1H – ^1H COSY spectra of cationic **TOL**–starch copolymers recorded on the AVANCE NEO-1.2 GHz spectrometer (Bruker, USA) operating at 1.2 GHz in $\text{DMSO-}d_6$. Reproduced from Zhao *et al.*²⁵ with the permission of Elsevier.

of **TOL**, and the APTAC monomer. It was also found that the phenolic hydroxyl content of **TOL** was reduced by the reaction of the APTAC chain with the phenolic OH of **TOL**, significantly increasing the solubility, charge density, and molecular weight of the cationic copolymers.

In 2023, Wang *et al.*²⁶ explored the free-radical *in situ* copolymerization study of lignin, acrylamide, and diallyldimethylammonium chloride by a combination NMR with other methods. It was shown that the presence of acrylamide in that reaction was essential for the polymerization of diallyldimethylammonium chloride with lignin to proceed due to the lower steric hindrance of the former (Fig. 8). The monomer conversion ratio and dynamic rheology of the reaction system indicated that lignin acted as an inhibitor in the corresponding copolymerization reaction.

Mun *et al.*²⁷ studied the samples of kraft lignin from mixed hardwoods by ^1H and ^{13}C NMR. It is well known that the basic aromatic structure of hardwood lignin consists of guaiacyl (**G**) and syringyl (**S**) units, both of which can be seen in the ^1H NMR spectra of acetylated kraft lignin (**Ac-KL**) and most clearly in the spectra of acetylated milled wood lignins (**Ac-MWL**) extracted from acacia (**Ac-MWL-aca**) and mixed hardwood (**Ac-MWL-mhw**) (see the marked yellow region in Fig. 9). The intensities of aromatic protons in **Ac-KL** were 0.52 for **S** and 0.37 for **G** units, while for **Ac-MWL-mhw**, the aromatic proton intensities were accordingly 0.84 for **S** and 0.57 for **G** units. Based on the ^1H NMR spectral intensities of **Ac-KL** and **Ac-MWLs**, the authors detected the decreased number of aromatic protons, suggesting a highly condensed structure of **KL**. As shown in Table 1, the **S/G** molar ratio of **Ac-KL** was almost similar to that of **Ac-MWL-mhw**.

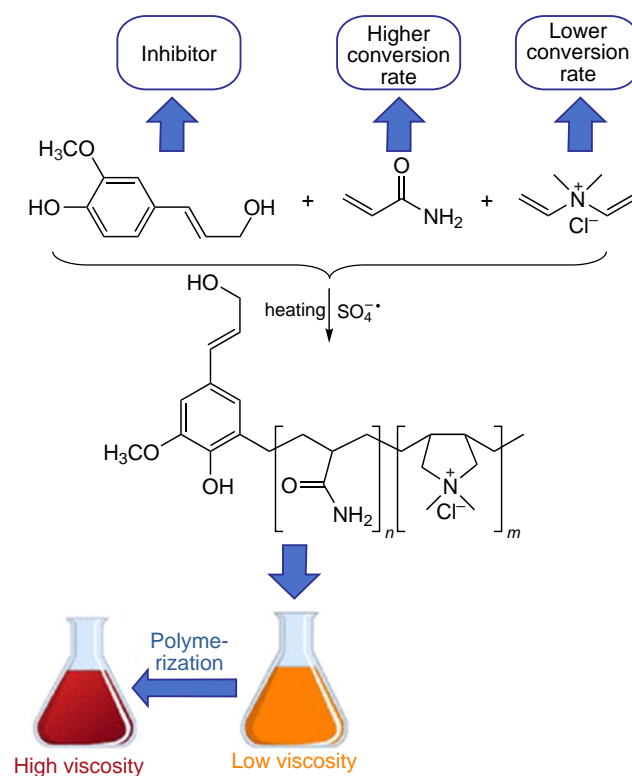


Figure 8. Copolymerization scheme of lignin, acrylamide, and diallyldimethylammonium chloride monitored by NMR. Reproduced from Wang *et al.*²⁶ under the Attribution-NonCommercial 4.0 International Public License (CC BY-NC 4.0).

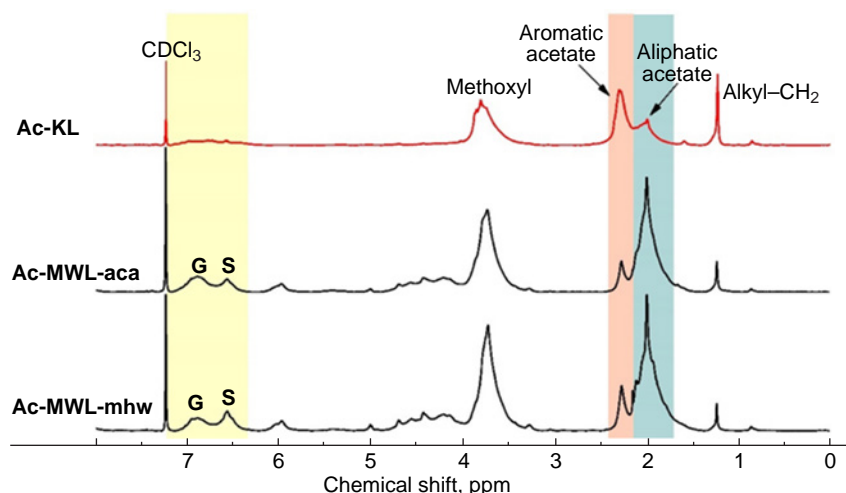


Figure 9. ^1H NMR spectra of acetylated kraft (**Ac-KL**) and milled wood (**Ac-MWL**) lignins recorded on a JNM-ECZ500R NMR spectrometer (JEOL, Japan) operating at 500 MHz in CDCl_3 . Reproduced from Mun *et al.*²⁷ under the Attribution-NonCommercial 4.0 International Public License (CC BY-NC 4.0).

Table 1. ^1H NMR assignments and fractions of protons of acetylated kraft and milled wood lignins.²⁷

Range, ppm	Structural unit	Integrated fraction		
		Ac-KL	Ac-MWL-aca	Ac-MWL-mhw
7.20–6.80	Aromatic protons (G units)	0.37	0.84	0.57
6.80–6.25	Aromatic protons (S units)	0.52	0.72	0.84
6.25–5.75	H_α of β -O-4 structures	–	0.31	0.33
4.90–4.30	H_α and H_β of β -O-4 structures	0.17	1.09	1.09
4.30–4.00	H_α of β - β structures, H of xylan residues	0.25	0.85	0.83
4.00–3.48	H of methoxyl groups	3.72	4.68	4.65
2.50–2.22	H of phenolic acetates	2.54	0.65	0.83
2.22–1.60	H of aliphatic acetates	2.22	5.33	5.42
1.40–0.70	Hydrocarbons (methyl groups)	0.76	0.31	0.19

Note. The dash means that no data are available.

The ^{13}C NMR spectra of **KL** and milled wood lignin (**MWL**) from acacia and mixed hardwood are presented in Figure 10. The corresponding chemical shifts and signal intensities are listed in Table 2. The ^{13}C NMR spectra of **MWL-aca** and **MWL-mhw** in aliphatic and aromatic regions were found to be essentially similar. However, the ^{13}C NMR spectrum of **KL** showed decreased aliphatic and increased aromatic content. This phenomenon was typical for **KL** since significant structural changes occurred in the aliphatic and aromatic moieties of lignin during kraft pulping. In addition, demethylation of methoxyl groups and cleavage along C_γ leading to polycondensation resulted in a marked difference between **KL** and **MWL** spectra,

Table 2. ^{13}C NMR assignments of kraft and milled wood lignins.²⁷

Chemical shift, ppm	Assignment ^a	Signal intensity ^b		
		KL	MWL-aca	MWL-mhw
195.7	C_γHO (7), C_α (15)	vw	vw	vw
192.6	C_α (9)	vw	vw	vw
171.5	Acetyl C=O in alcohols and/or phenols	–	w	m
162.5	C-4 in <i>p</i> -hydroxybenzoate	–	m	m
153.4	C-3/C-5 (3b)	w	s	vs
150.2	C-4 (2b), C-3 (2d)	–	w	w
148.2	C-3 (2a, 2b, 2e, 2f), C-3/C-5 (3a), C-3 (5)	vs	m	m
146.3	C-4 (2a), C_α (6)	w	w	w
144.6	C-4 (4)	w	w	w
138.5	C-1/C-4 (3b)	–	m	m
135.4	C-1 (2b), C-4 (3a)	–	m	m
133.6	C-1 (1a, 2a, 3a)	s	w	w
132.5	C_β (7)	s	w	w
129.9	C-1 (2e, 4)	m	vw	vw
129.0	C-2/C-6 (1), C_β (8)	w	vw	vw
126.6	C-6 (2d)	m	–	–
120.3	C-6 (2a, 2b)	m	m	m
115.5	C-5 (2a, 2b), C-3/C-5 (1)	s	m	m
111.9	C-2 (2a, 2b)	w	m	m
109.9	C-6 (2a, 2b)	w	–	–
107.0	C-2/C-6 (3c, 3d)	w	w	w
104.9–103.8	C-2/C-6 (3a, 3b)	s	m	s
88.1	C_α (12)	–	w	w
86.6	C_α (13), C_β (10)	–	w	m
86.3	C_β (10)	–	w	m
83.4–81.0	C_β (15)	–	w	w
75.0	C_α (11)	w	w	w
73.3	C_α (10, 13, 15)	w	s	s
63.6	C_β (11), C_γ (8, 11, 12, 15)	w	s	s
61.2	C_γ (10)	–	s	s
56.4	OCH_3	vs	vs	vs
20.8	Acetyl CH_3	vw	w	m

^a Enumeration of lignin substructures and side chains (bold arabic numbers) is provided in Figure 10; ^b the designations are as follows: w is weak, s is strong, m is medium, vw is very weak, vs is very strong. The dash means that no data are available.

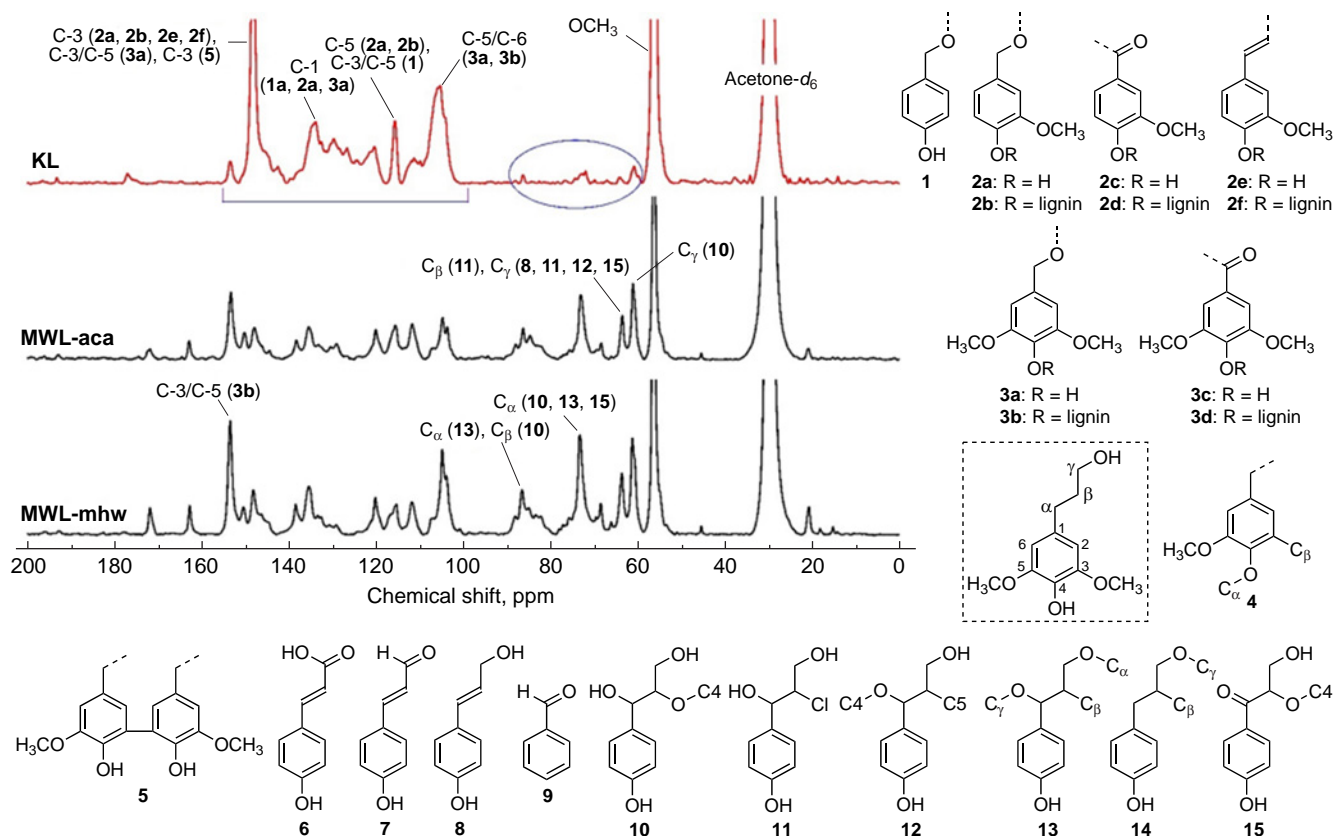


Figure 10. ^{13}C NMR spectra of kraft lignin and milled wood lignin recorded on a JNM-ECZ500R NMR spectrometer (JEOL, Japan) operating at 125 MHz in CDCl_3 . List of substructures **1–5** and side chains **6–15** of lignin and numbering of carbon atoms in the base fragment (highlighted with dotted lines). Reproduced from Mun *et al.*²⁷ under the Attribution-NonCommercial 4.0 International Public License (CC BY-NC 4.0).

as was claimed by the authors as one of the main results of their study.

Rönnols *et al.*²⁸ discussed the prospects for lignin analysis by the low-field benchtop NMR spectroscopy. It is well known that benchtop NMR spectroscopy is an emerging field with an appealing profile for analytical analysis of lignin. The instrumentation of the benchtop NMR spectroscopy offers the possibility to measure NMR spectra in situations where the use of the high-field NMR spectroscopy is too expensive or unavailable. In that paper, the ability to quantify different lignin samples using benchtop NMR was found to be rather promising. For example, the ^1H NMR spectra of isolated lignin samples recorded at benchtop low and high magnetic fields showed three major peaks arising from aromatic and oxygenated aliphatic compounds together with that of the residual solvent with the corresponding spectral regions being clearly separated (Fig. 11).

2.2. ^1H and ^{13}C two-dimensional NMR

Two-dimensional NMR of lignin is currently used as either a qualitative or a semi-quantitative technique. An example of this is the fundamental study by Levdansky *et al.*,²³ who used HSQC spectra to confirm the presence of the $\beta\text{-O-4}'$, $\beta\text{-}\beta'$, and $\beta\text{-5}'$ linkages in the organosolv lignin extracted from fir and aspen, as shown in Figures 12 and 13. The main structural units of these ethanol lignins are also presented (see Fig. 12).

The same year, Li *et al.*²⁹ reported a kinetic study of the hydrogenolysis of lignin to monomers in a continuous flow reactor using 2D HSQC NMR spectra (Fig. 14). It was found that lignin end and internal units reacted essentially differently

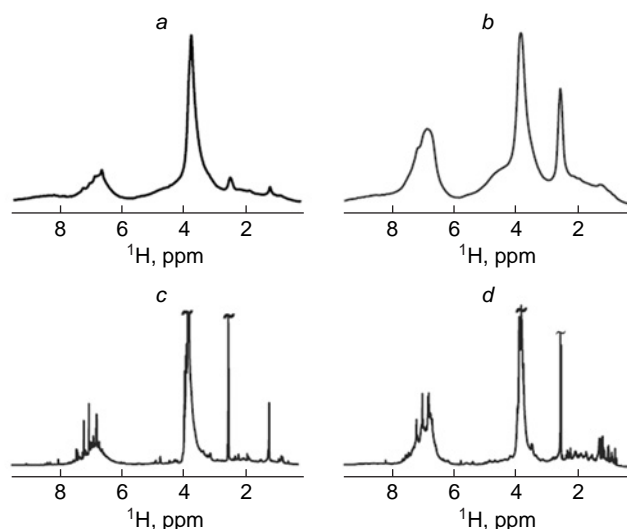


Figure 11. ^1H NMR spectra of the isolated lignin samples recorded at low and high magnetic field strengths (43 and 60 MHz): the hardwood lignin sample at low field (*a*) and high field (*c*); softwood kraft lignin sample at low field (*b*) and high field (*d*). Spectra were recorded in $\text{DMSO-}d_6$ using two benchtop NMR systems, Spinsolve 43 MHz Diffusion and Spinsolve 60 MHz Ultra (Magritek, Aachen, Germany), generating magnetic field strengths of 1 and 1.5 T, respectively. Reproduced from Rönnols *et al.*²⁸ with the permission of Walter/De Gruyter GMBH & Co, KG.

which provided insight into lignin hydrogenolysis pathways. As a result of that study, a continuous lignin upgrading process was

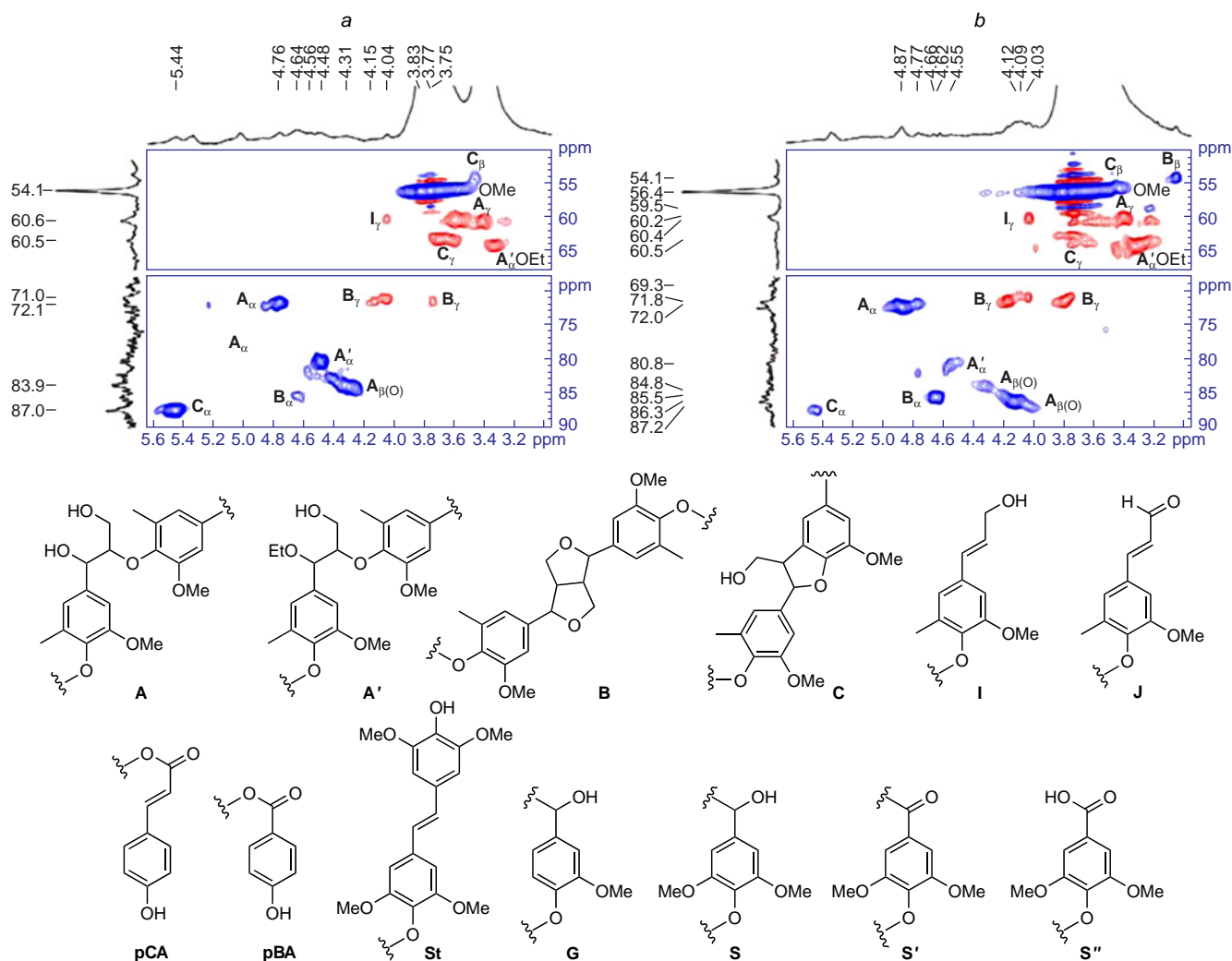


Figure 12. Aliphatic region of the HSQC spectra of ethanol lignins extracted from fir (a) and aspen (b). All $^1\text{H}/^{13}\text{C}$ NMR spectra were recorded on a Bruker Avance 600 NMR spectrometer operating at 600/150 MHz in $\text{DMSO-}d_6$. The main structural units of ethanol lignins extracted from fir and aspen wood: **A** is β -aryl ethers, **A'** is α -ethoxylated β -aryl ethers, **B** is pinosresinol, **C** is phenylcoumarans, **I** is terminal cinnamic alcohol groups, **J** is terminal cinnamic aldehyde groups, **pCA** is *p*-coumarates, **pBA** is *p*-hydroxybenzoates, **St** is stilbenes, **G** is guaiacyl units, **S** is syringyl units, **S'** and **S''** is oxidized syringyl units (c). Reproduced from Levdansky *et al.*²³ with the permission of the Siberian Federal University.

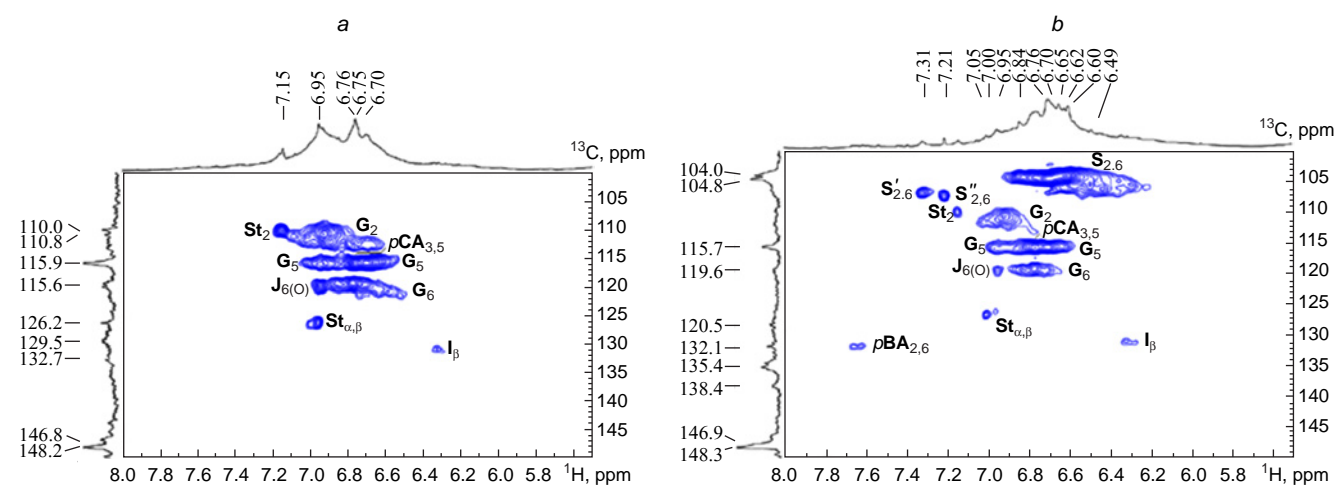


Figure 13. Aromatic region of the HSQC spectra of ethanol lignins extracted from fir (a) and aspen (b). All $^1\text{H}/^{13}\text{C}$ NMR spectra were recorded on a Bruker Avance 600 NMR spectrometer operating at 600/150 MHz in $\text{DMSO-}d_6$. Reproduced from Levdansky *et al.*²³ with the permission of the Siberian Federal University.

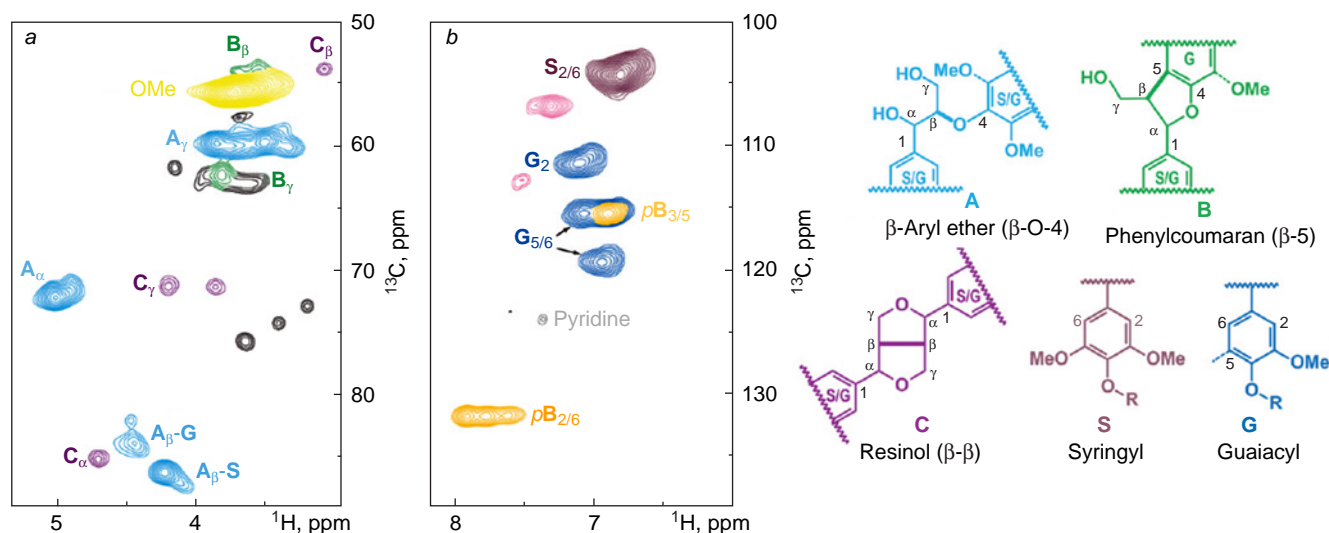


Figure 14. Partial 2D HSQC NMR spectra of copper-catalyzed alkaline hydrogen peroxide (Cu-AHP) lignin obtained from poplar — Cu-AHP lignin hydrogenolysis products after flow-tube reaction: lignin sidechain fingerprint region (a); aromatic region (b). NMR spectra were recorded in DMSO- d_6 /pyridine- d_5 on a Bruker Biospin AVANCE-III 700 MHz spectrometer fitted with a cryogenically-cooled 5 mm gradient probe. Reproduced with minor editing privileges from Li *et al.*²⁹ with the permission of the Royal Society of Chemistry.

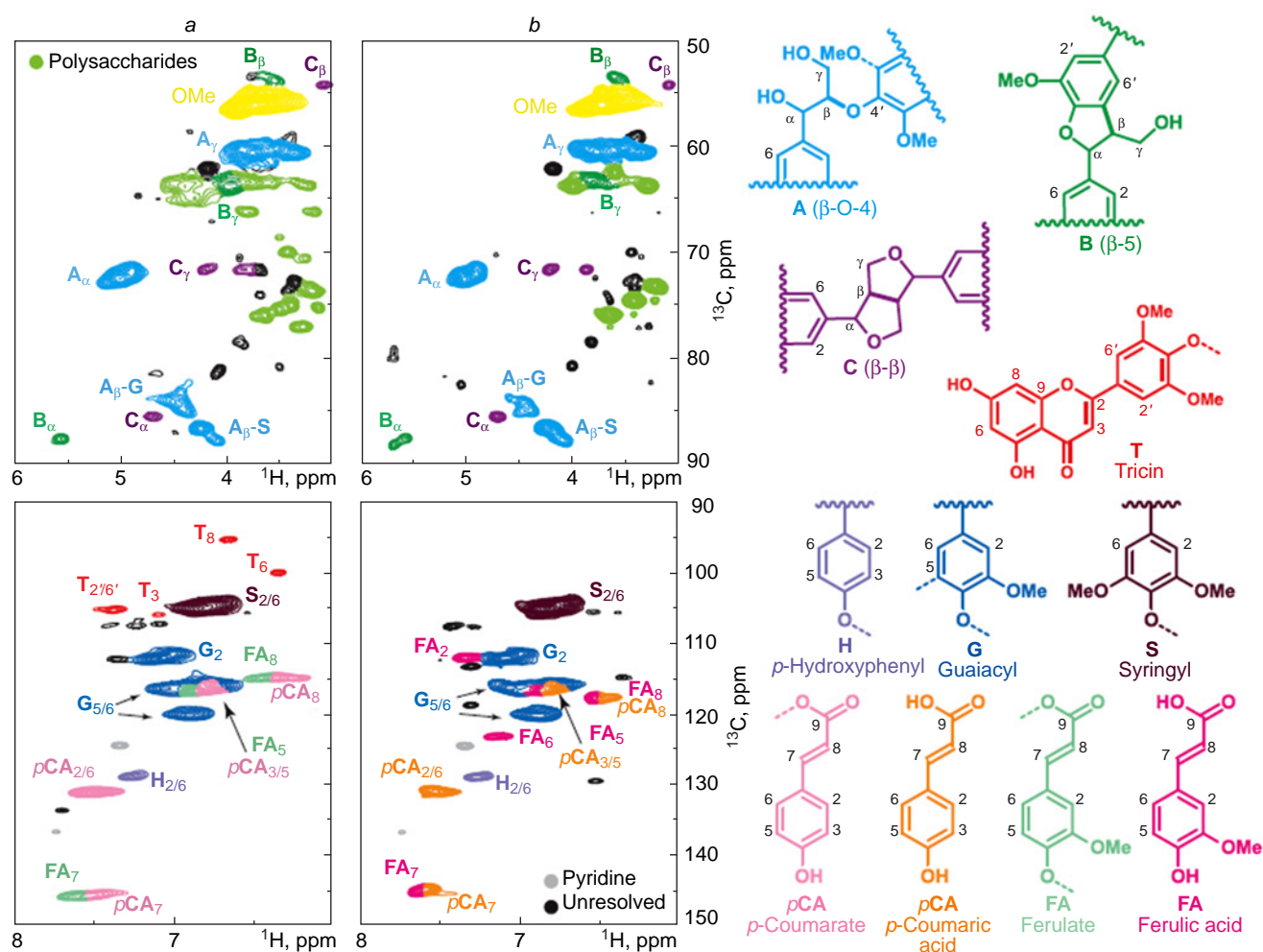


Figure 15. Partial 2D HSQC NMR spectra of reed straw enzyme lignins and alkali-pretreated reed lignin (1% NaOH). The retained polysaccharides are mainly xylan in the alkali-soluble lignin. For details, see original publication. NMR spectra were recorded in DMSO- d_6 /pyridine- d_5 on a Bruker Biospin AVANCE-III 700 MHz spectrometer fitted with a cryogenically-cooled 5 mm gradient probe. Reproduced from Liu *et al.*³⁰ with minor editing privileges under the Attribution-NonCommercial 4.0 International Public License (CC BY-NC 4.0).

developed using soluble lignin in a continuous flow reactor. The advantages of the flow-through system included the continuous production of lignin monomers monitored by 2D HSQC NMR by optimizing reaction parameters such as reaction temperature, pressure, and flow-rate in real time.

The resulting 2D HSQC NMR spectra showed that the major lignin sidechain units (β -O-4, β -5, and β - β) in the Cu-catalyzed alkaline hydrogen peroxide (Cu-AHP) lignin were well resolved in the sidechain fingerprint region. The aromatic signals were similar to those from kraft lignin, except for a small amount of the benzylic oxidation caused by the Cu-AHP pretreatment. The signals of the lignin side-chain units showed no obvious changes before and after the reaction.

In 2019, Liu *et al.*³⁰ reported a rapid lignocellulose fractionation method applied to common reed based on milling

under mild alkaline conditions with using no organic solvents or other reagents. As a result, the lignin-containing cellulose nanofibre and native-like lignins were obtained. Films prepared from the suspension of the lignin-containing cellulose nanofibres showed very interesting properties such as transparency and hydrophobicity. Shown in Figure 15 are characteristic partial 2D HSQC NMR spectra of reed straw enzyme and alkali-pretreated reed lignins. Overall, the isolated lignin preserved its native structure with high β -ether content. The resulting isolated high-quality lignin was found to be suitable for further upgrading by various lignin depolymerization processes.

Wang *et al.*³¹ developed an integrated process based on hydrothermal pretreatment and Kraft delignification to deconstruct lignocellulosic biomass. Hydrothermal pretreatment was found not only to facilitate the production of *xylo-*

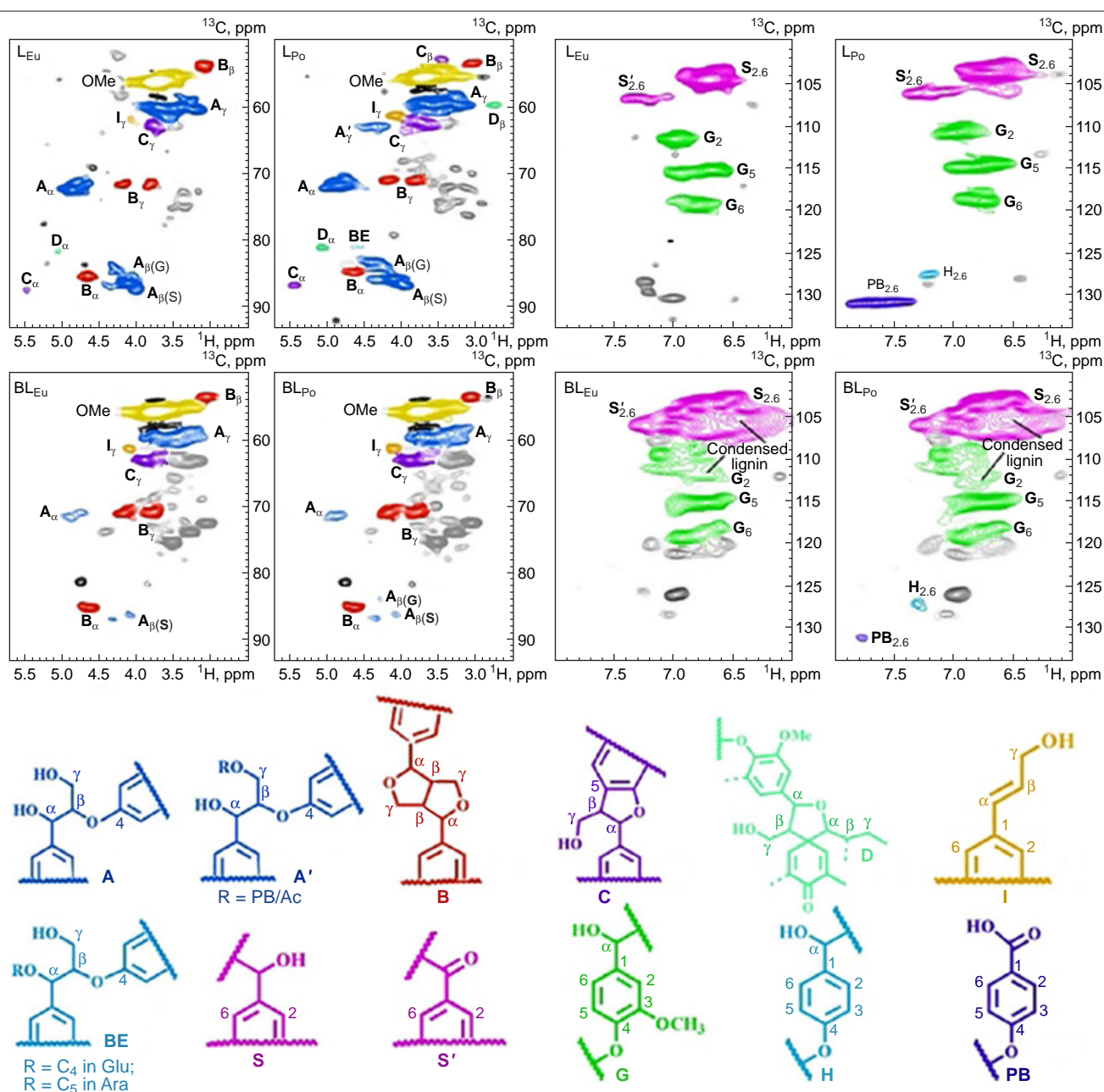


Figure 16. Side-chain and aromatic regions in 2D HSQC NMR spectra of lignins obtained from raw materials and corresponding black liquor. For details, see original publication. NMR spectra were recorded on a Bruker AVIII 400 MHz spectrometer in DMSO-*d*₆. BE is benzyl ether, PB is *p*-hydroxybenzoate. Reproduced from Wang *et al.*³¹ with the permission of Wiley.

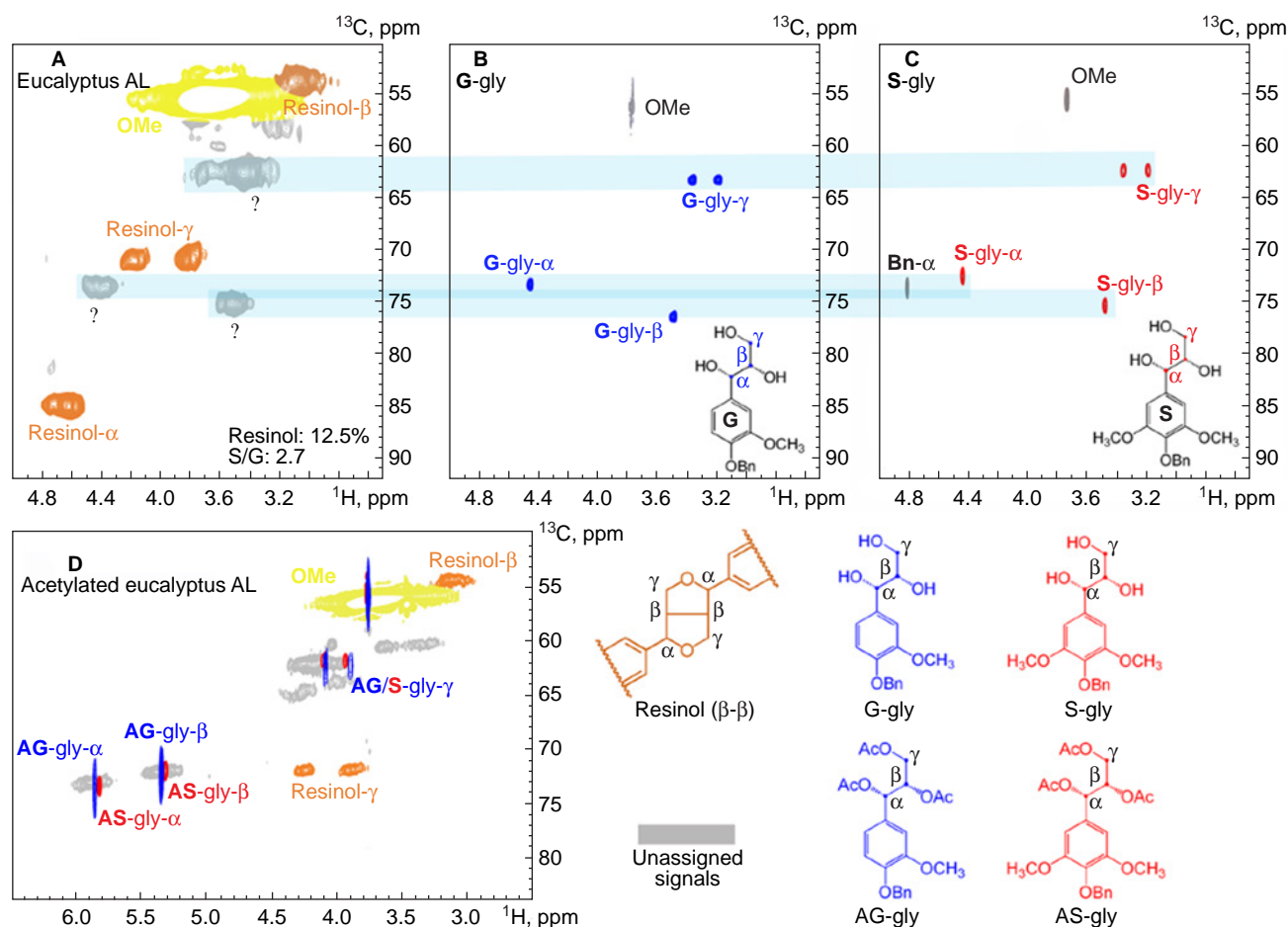


Figure 17. Partial 2D HSQC NMR spectra of nonacetylated/acetylated eucalyptus alkaline lignin (AL) and phenylglycerol compounds for peak assignment. The unknown peaks in (A) of eucalyptus AL were compared to the peaks in (B) from G-gly and (C) S-gly. The phenylglycerol structure in AL was also confirmed by matching the peaks from acetylated compounds and acetylated AL (D). For details, see original publication. NMR spectra were recorded on a Bruker AVANCE III HD 600 MHz spectrometer in DMSO- d_6 . Reproduced from Zhao *et al.*³² with the permission of the American Chemical Society.

oligosaccharides but also to reduce the chemicals dosage of the following delignification. The structural characteristics of lignin obtained from the integrated process were studied by 2D HSQC NMR (Fig. 16).

Zhao *et al.*³² prepared alkaline and kraft lignins and carried out their comparative characterization by 2D HSQC NMR (Figs 17 and 18). Using authenticated reference compounds, the phenylglycerol structures, characteristic of the cleavage of non-phenolic β -aryl ether by soda pulping, in the alkaline lignin were identified and quantified by 2D HSQC NMR. The content of phenylglycerol compounds in alkaline lignin was estimated to be 8–14%, which was much higher than that in kraft lignin.

A large number of related 2D HSQC NMR studies have recently appeared devoted to the structural studies of lignin and lignin-related products, as exemplified below being among many other related papers.

Cao *et al.*³³ investigated the microwave-assisted depolymerization of various types of waste lignins elucidating how the structure of lignins recovered from various agricultural and industrial residues affects its downstream catalytic conversion. Three types of lignins, such as bio-enzymatic lignin, organosolv lignin, and Kraft lignin, were fully characterized by HSQC-NMR to obtain a detailed description of their structures, as shown in Figure 19. The strong dependence of the conversion efficiency on the interunit linkages and functional groups of

lignin structures was found. The strong metal–support interaction between CuO and sodium cyanoborohydride NaBH₃CN not only facilitated lignin depolymerization *via* the promoted electron transfer, but also improved the stability of Cu catalysts under hydrothermal conditions.

Chen *et al.*³⁴ developed an integrated biorefinery strategy towards phenolics, levulinic acid, and furfural during total utilization of lignin and carbohydrates in *Eucalyptus grandis*. It is well known that the depolymerization of lignin into the well-defined mono-aromatic chemicals suitable for downstream processing is recognized increasingly as an important starting point for the lignin valorization. In that study, the conversion of all three components of *Eucalyptus grandis* into the corresponding monomeric chemicals was investigated using solid and acidic catalysts in sequence. The 2D HSQC NMR spectra of the lignin oil shown in Figure 20 confirmed that the main substructures, such as β -aryl ether (β -O-4), resinol (β - β), and phenyl coumaran (β -5) have disappeared after Pd/C treatment, indicating the C–O bonds dissociation in protolignin. New dominant cross peaks corresponding to a propanol moiety were observed in HSQC. The cross signals in the aromatic region corresponding to guaiacyl and syringyl units were also found.

Kim *et al.*³⁵ carried out a 2D HSQC study of monolignol benzoates incorporation into the lignin of transgenic *Populus*

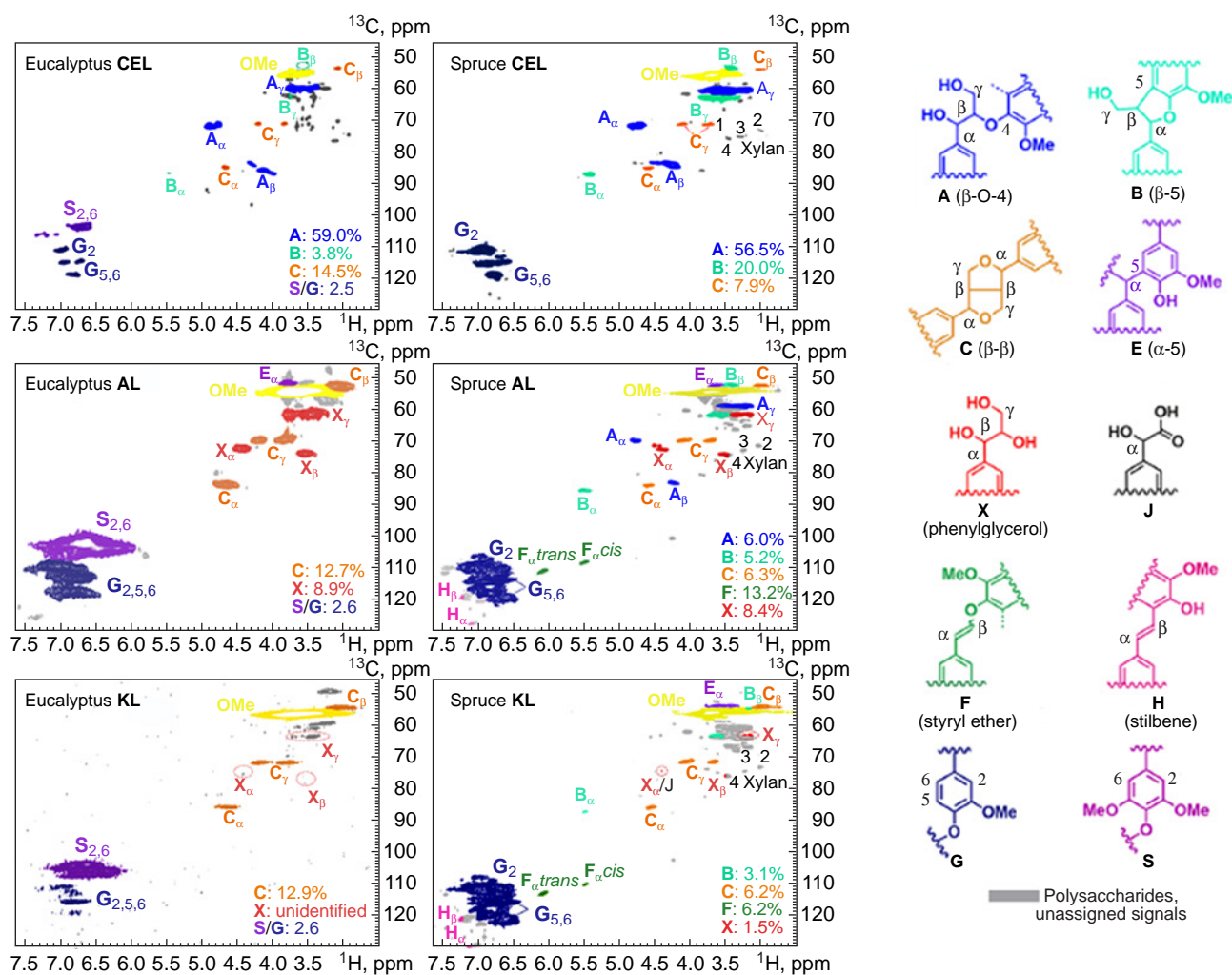


Figure 18. Partial 2D HSQC NMR spectra of enzyme lignin (CEL), alkaline lignin (AL), and kraft lignin (KL) of spruce and eucalyptus. For details, see original publication. NMR spectra were recorded on a Bruker AVANCE III HD 600 MHz spectrometer in DMSO- d_6 . Reproduced from Zhao *et al.*³² with minor editing privileges with the permission of the American Chemical Society.

trichocarpa (Fig. 21). It was found that monolignol benzoates incorporated into the lignin of triple-transgenic *Populus trichocarpa*, which is downregulated for the three endoplasmic reticulum cytochrome enzymes participating in oxidative radical coupling reactions during lignification in the cell wall. This study has demonstrated how the biosynthesis of monolignol benzoate and monolignol *p*-hydroxybenzoate in plant is involved in the lignin biosynthetic pathway by providing direct evidence for the monolignol benzoate and monolignol *p*-hydroxybenzoate structures in the transgenic *Populus trichocarpa* lignin. In addition, attention was drawn to the convoluted interactions of enzymes in the pathway to produce benzoates.

Li *et al.*³⁶ used a number of methods to identify the biomass structural determinants defining the properties of the plant-derived renewable carbon fibre. The linkages and composition of lignin from eight sorghum feedstocks were analyzed by 2D HSQC NMR and the linkage profiles of uncondensed β -O-4, condensed β -5, and condensed β - β were calculated based on a number of aromatic rings of syringyl, guaiacyl and *p*-hydroxyphenyl units. At that, the frequencies of β -O-4, β -5, and β - β linkages were determined based on a series of 2D HSQC NMR experiments (Figs 22 and 23). Considering the diverse range of lignin characteristics, lignin from the sorghum feedstock samples was found to be a perfect model precursor to elucidate the impact of biomass characteristics on the performance of the

resultant carbon fibres. That 2D HSQC NMR study opened a new path to modify cell wall structures for manufacturing the high-quality carbon fibres.

Liu *et al.*³⁷ reported the method for isolation and characterization of crude lignin of bark using the ethanol-water organosolv treatment. According to the two-dimensional ^1H - ^{13}C 2D HSQC NMR and monodimensional ^{13}C NMR spectral data, crude lignin contained mixed polyphenolics, suberin compounds and carbohydrates (Fig. 24). Overall, this study demonstrated the potential to solubilize a high proportion of bark and provided insight into the structure–property relationships of crude lignin as a function of processing conditions.

Rowlandson *et al.*³⁸ investigated the influence of aromatic structure of lignin on its thermal behaviour. The authors performed a systematic study of the chemical composition of lignins extracted using an identical organosolv isolation method but from different biomass feedstocks: hemp hurds, eucalyptus chips, flax straw, rice husk and pine. Basic results were obtained mainly from the 2D-NMR HSQC spectra shown in Figure 25 for rice husk lignin, eucalyptus lignin and industrial lignin. It was found how the aromatic structure of lignin could affect the thermal behaviour of the polymer, which correlated with the structure of the resulting carbons. Carbons from lignins with a high content of syringyl units displayed a pronounced foaming

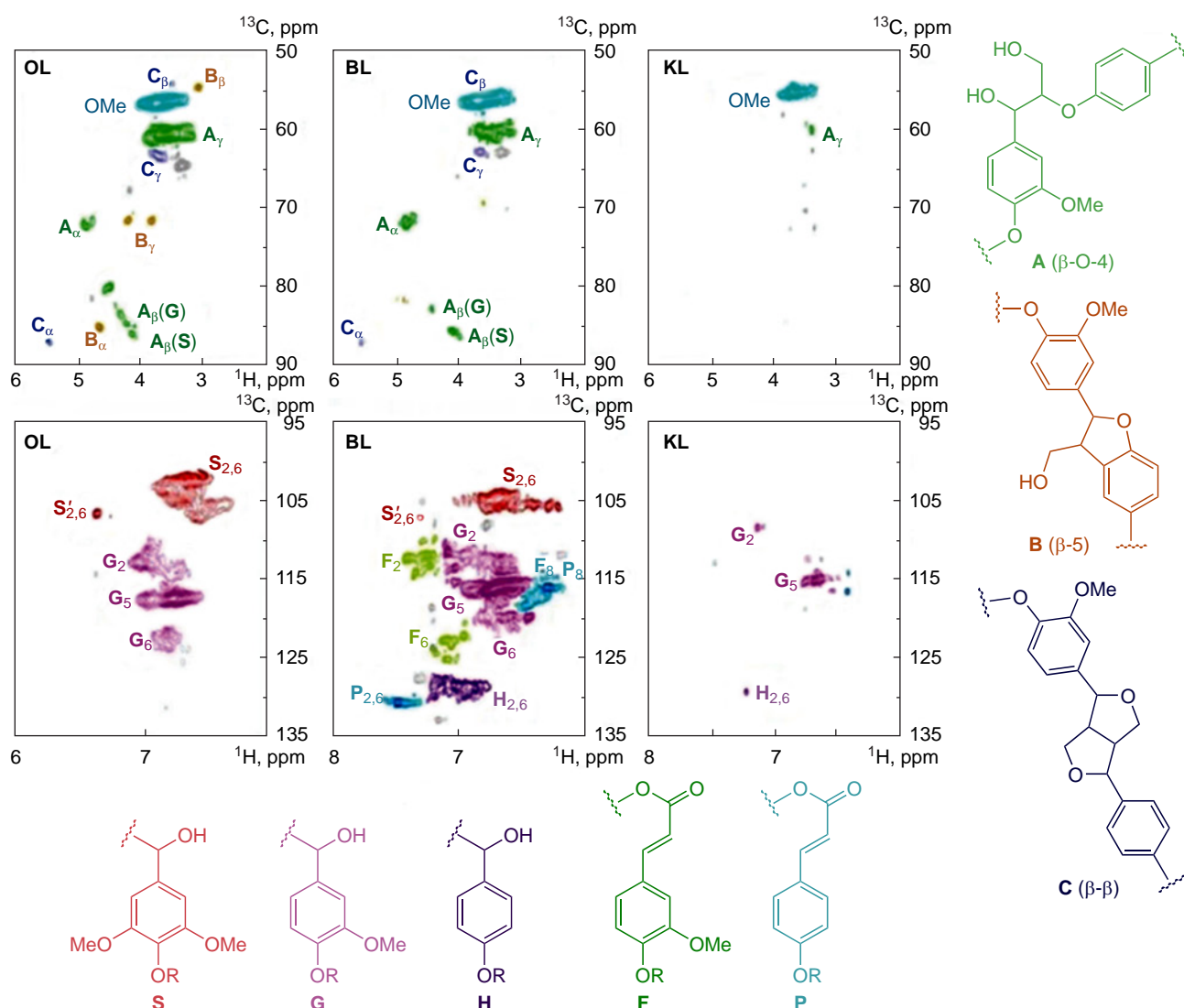


Figure 19. Side-chain and aromatic regions in 2D HSQC NMR of various lignin samples: bioenzymatic lignin (BL), organosolv lignin (OL) and Kraft lignin (KL). The main substructures identified by 2D NMR: A is β -O-4 linkage; B is β -5 linkage; C is β - β linkage; S is syringyl unit; G is guaiacyl unit; H is *p*-hydroxyphenyl unit; F is ferulic acid unit and P is *p*-coumaric acid unit. 2D HSQC NMR spectra of various types of lignins were recorded on a Bruker AVIII 400 MHz spectrometer. About 80 mg of lignin was dissolved in 0.6 mL of $\text{DMSO-}d_6$. Reproduced with minor editing privileges from Cao *et al.*³³ with the permission of the Royal Society of Chemistry.

behaviour which, upon activation, resulted in a high-surface area material with hierarchical porosity.

It was found that organosolv lignin samples contained syringyl unit, oxidized syringyl unit, guaiacyl unit, *p*-hydroxyphenyl unit, ferulic acid, cinnamyl alcohol end group, cinnamaldehyde end group, and *p*-coumaric acid with the following main linkages present: β -aryl-ether β -O-4, resinol β - β , phenylcoumaran β -5 and spirodienone (Fig. 26).

Tokunaga *et al.*³⁹ explored the nonproductive binding sites of lignin models with carbohydrate-binding module of cellobiohydrolase. In this study, three types of ^{13}C -labeled β -O-4 lignin oligomer models were synthesized and characterized. According to the 2D ^1H - ^{13}C HSQC spectra of the ^{13}C -labeled lignin models (Fig. 27), three types of the ^{13}C labels were correctly incorporated in the aromatic rings and β -positions, α -positions and methoxy groups. The *Trichoderma reesei* carbohydrate-binding module 1 (*Tr*CBM₁) binding sites in lignin were analyzed by observing NMR chemical shift perturbations using the synthetic ^{13}C -labeled β -O-4 lignin oligomer models. Obvious chemical shift perturbations were

found in signals from the aromatic regions in oligomers bound to *Tr*CBM₁, whereas changes in the signals from aliphatic regions and methoxy groups were insignificant. These results suggested that hydrophobic interactions and π - π stacking were dominating factors in the nonproductive binding.

Ghavidel *et al.*⁴⁰ studied chemical reactivity and sulfonation of enzymatically produced lignin. The comparison between six different enzymatically hydrolyzed lignin samples revealed the fundamental role of β -aryl ether and residual carbohydrate on the physicochemical properties and chemical reactivity of the samples used to generate dispersants for the clay suspension. Based on the 2D HSQC spectra of six hydrolyzed lignin samples shown in Figure 28, it was established that lignin samples with fewer β -O-4 and lignin-carbohydrate bonds (LCC) had a higher content of Ph-OH and carboxylate groups. The higher ratio of these bonds was associated by the authors with the superior contribution of the β -aryl ether and lignin-carbohydrate bonds. The samples with the lower sugar content appeared to be smaller and more porous, which increased the chemical

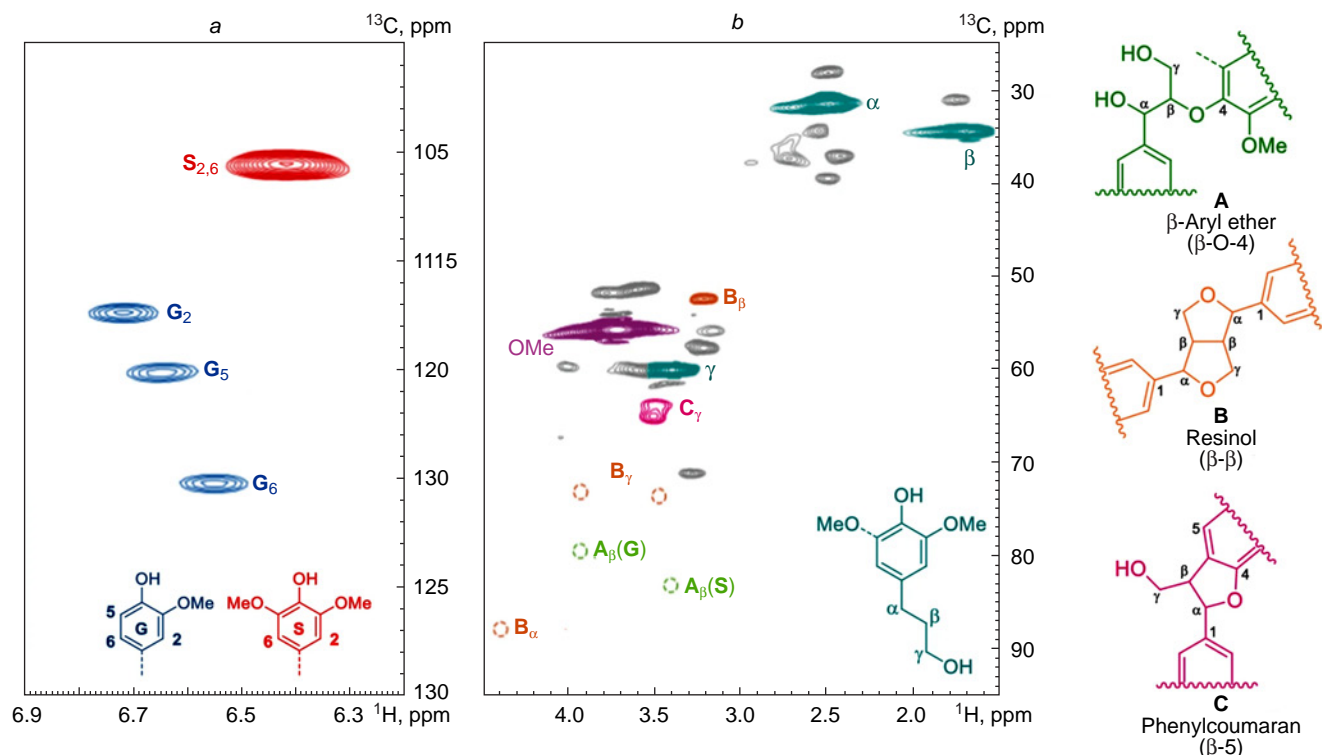


Figure 20. 2D HSQC NMR spectra of the lignin oil obtained at 240°C, 4 h ($\text{DMSO-}d_6$). Aromatic region (a). The signals from the G and S units appeared at 112.2/6.71 (G_2), 115.0/6.64 (G_5), 120.0/6.55 (G_6) and 105.4/6.41 ($\text{S}_{2,6}$) ppm, respectively. Side chain region (b). The signals from the propanol moiety were found at 31.7/2.49, 34.5/1.68 and 60.1/3.40 ppm, respectively. 2D HSQC NMR spectra were recorded on a Bruker Avance 400 MHz spectrometer in $\text{DMSO-}d_6$. Reproduced from Chen *et al.*³⁴ under the Attribution-NonCommercial 4.0 International Public License (CC BY-NC 4.0).

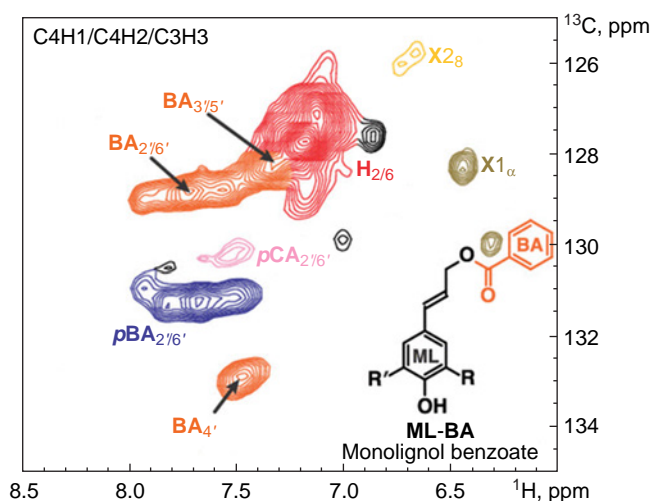


Figure 21. Aromatic region of 2D HSQC NMR spectra ($\text{DMSO-}d_6$ /pyridine- d_5 , 4:1, v/v) of enzyme lignins isolated from *Populus trichocarpa* and C4H/C3H-downregulated transgenics. 2D HSQC NMR spectra were recorded on a Bruker Biospin Avance 700 MHz spectrometer equipped with a 5 mm cryoprobe with inverse geometry in $\text{DMSO-}d_6$ /pyridine- d_5 (4:1, v/v). Reproduced from Kim *et al.*³⁵ under the Attribution-NonCommercial 4.0 International Public License (CC BY-NC 4.0).

reactivity of the hydrolyzed lignin by making it more accessible to the functionalization reactions.

Islam *et al.*⁴¹ used *N*-methyl-2-pyrrolidone (NMP) pretreatment of lignocellulose to increase lignin yield and cellulose digestibility. The authors discovered a new *N*-methyl-

2-pyrrolidone pretreatment solvent with excellent lignin solubility and preservation of β -O-4 linkages present in the pristine lignin structure. These results indicated that the formation of 4-(methylamino)butyric acid in the NMP pretreatment system increased the polarity of the solvent system. The increased polarity in turn increased the lignin removal and reduced the amount of lignin condensation. This result was attributed to the higher amount of the β -O-4 interunit linkages in the NMP lignin sample, which was mainly determined by HSQC analysis.

The ^1H - ^{13}C 2D HSQC NMR spectra shown in Figure 29 demonstrated that the major substructures of the studied lignin were S and G units together with interunit β -O-4, β - β and β -5 linkages. The NMR signals were assigned by comparison with those of the benchmark ball mill lignin. The position and colour of the correlations shown represent the corresponding substructures, which are β -O-4 (green), β -5 (brown), and β - β (pink), S unit (grass green), G unit (light orange) and H unit (purple). The semi-quantitative values of major lignin moieties were determined using the aromatic units as an internal standard. For the ball milled lignin, α -position of β -O-4, β - β , and β -5 linkages appeared at $\delta_{\text{C}}/\delta_{\text{H}}$ 72.56/4.82 ppm, $\delta_{\text{C}}/\delta_{\text{H}}$ 85.66/4.60 ppm and $\delta_{\text{C}}/\delta_{\text{H}}$ 86.1/4.1 ppm, respectively. With the NMP pretreatment, the corresponding peaks were observed at the same position with different intensities. The β -O-4 was found to be the predominant linkage of the studied lignin, which determined the integrity and potential of fractionated lignin for its effective valorization to produce aromatic chemicals.

Diaz-Baca *et al.*⁴² carried out the polymerization of tall oil lignin, starch and 2-methyl-2-propene-1-sulfonic acid sodium salt to produce flocculants for colloidal systems together with

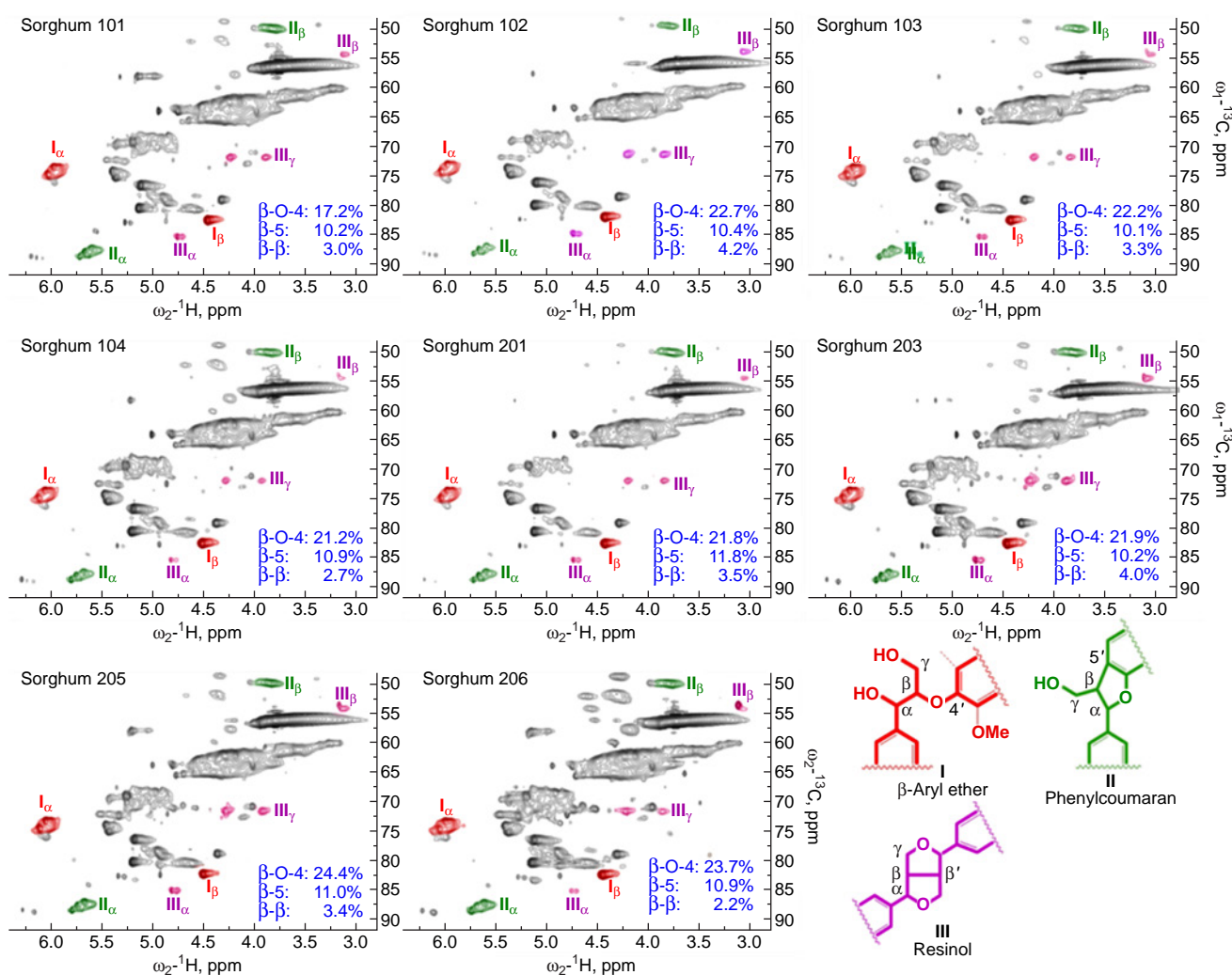


Figure 22. Internunitary linkages in the sorghum lignin as revealed by 2D HSQC NMR. Normalized lignin content in the samples: low (<0.3, Sorghum 103, 205), moderate (0.5–0.9, Sorghum 101, 104, 201, 206), high (>0.9, Sorghum 103, 205). Lignin (30–50 mg) was dissolved in 0.6 mL of DMSO- d_6 and placed in an NMR tube. Adiabatic 2D $^1\text{H}/^{13}\text{C}$ HSQC spectra were acquired on a Bruker Avance-III 400 MHz spectrometer equipped with a 5 mm broadband probe with a Z-gradient probe, Bruker). Reproduced from Li *et al.*³⁶ under the Attribution-NonCommercial 4.0 International Public License (CC BY-NC 4.0).

the sulfonated lignin–starch polymer, and described the use of the latter as a flocculant. Based on the advanced ^1H , COSY, HSQC, HSQC-TOCSY, and HMBC NMR techniques (Figs 30 and 31), it was confirmed that the phenolic substructures of tall oil lignin and the anhydroglucose unit of starch were covalently polymerized by the monomer to give the three-block copolymer.

Karlsson *et al.*⁴³ studied lignin structure and reactivity in the organosolv process. The aim of this work was to study the reactivity of lignin during a cyclic organosolv extraction process while using physical protection strategies. Synthetic lignins obtained by mimicking the lignin polymerization process were used as reference compounds. The authors used state-of-the-art NMR analysis, which is a powerful tool for elucidating lignin interunit linkages and functionalities. This study revealed interesting fundamental aspects of lignin polymerization, such as identifications of molecular populations with high degrees of structural homogeneity and the emergence of branching points in the lignin structure. Analysis of the organosolv biorefinery lignin by HSQC NMR, as exemplified in Figure 32, showed an abundance of aryl-ether linkages (β -O-4), confirming that physical protection did indeed occur due to performing the

extraction in cyclic mode. A previously proposed intramolecular condensation reaction was substantiated, and new insights into the selectivity of this reaction were introduced, which was supported by the density functional theory (DFT) calculations (Figs 33 and 34), where the important role of intramolecular π - π stacking was emphasized.

Rinken *et al.*⁴⁴ investigated the role of solvent fractionation of lignin oil in structural profiling during lignin stabilization, and the carbohydrate nature in the H-transfer reductive catalytic fractionation was also evaluated. In particular, the solvent fractionation of the reductive catalytic fractionation lignin oil was studied as a facile method for producing lignin oil fractions for advanced characterization. Solvent fractionation is known to use small volumes of environmentally benign solvents like methanol, acetone, and ethyl acetate to produce multigram lignin fractions containing products in different molecular weight ranges. This feature allows the determination of structural heterogeneity across the entire molecular weight distribution of the reductive catalytic fractionation lignin oil by high-resolution HSQC NMR spectroscopy. Performed study provided a detailed insight into the role of the hydrogenation catalyst in stabilizing

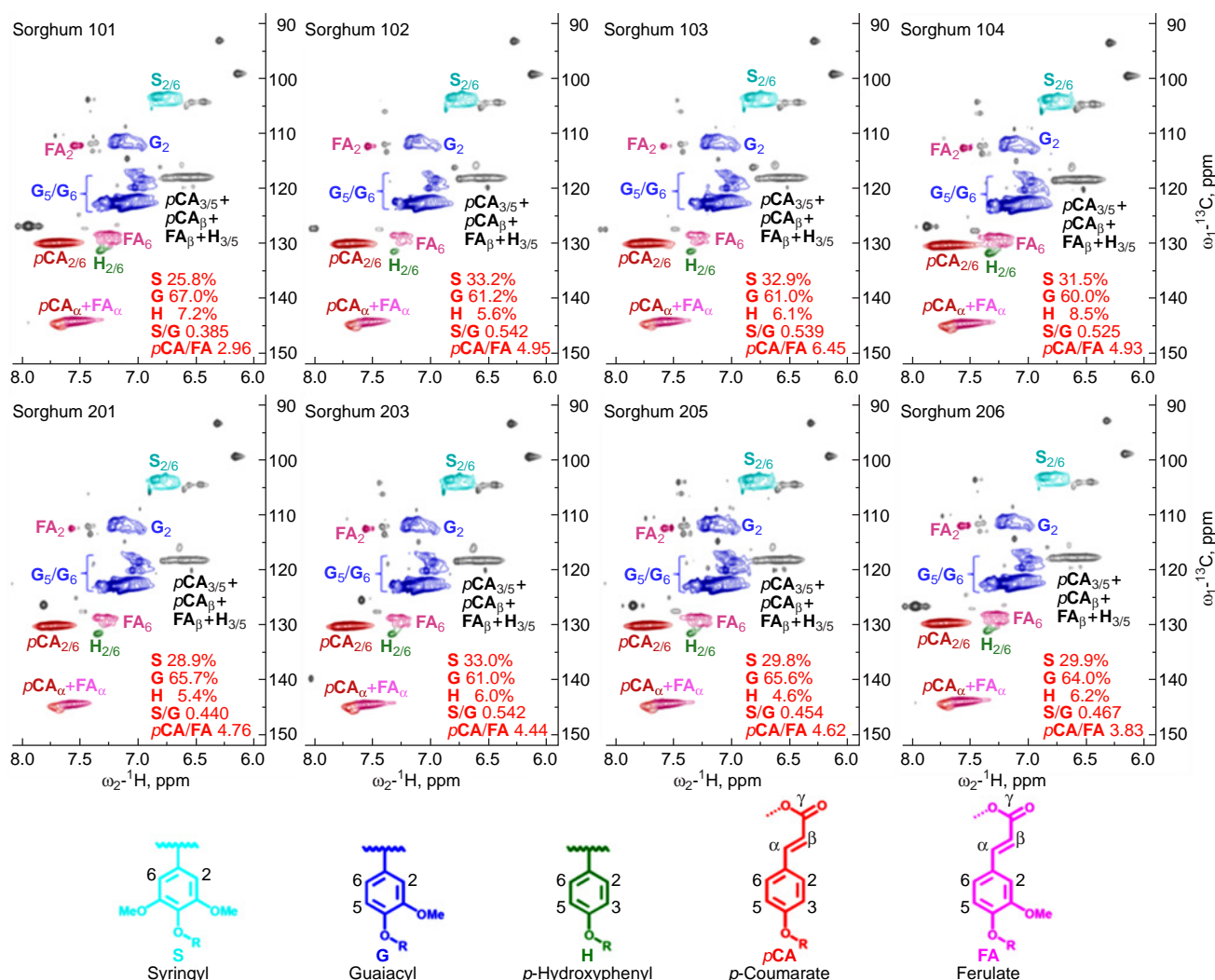


Figure 23. Aromatic regions of the 2D HSQC NMR spectra of lignin. **G₂**, **G₅** and **G₆** are carbon-2, carbon-5, and carbon-6 correlations from guaiacyl (**G**) units; **S_{2/6}** is carbon-2 and carbon-6 correlations from syringyl (**S**) units; **H_{2/6}** is carbon-2 and carbon-6 correlations from *p*-hydroxyphenyl (**H**) units; **pCA_{2/6}** and **pCA_α** are carbon-2 and carbon-6, and carbon- α correlations from *p*-coumarate (**pCA**) units; **FA₂**, **FA₅** and **FA_α** are carbon-2, carbon-5, and carbon- α correlations from ferulate (**FA**) units. For more details, see original publication. Lignin (30–50 mg) was dissolved in 0.6 mL of DMSO-*d*₆ and placed in an NMR tube. Adiabatic 2D ¹H/¹³C HSQC spectra were acquired on a Bruker Avance-III 400 MHz spectrometer equipped with a 5 mm broadband probe with a Z-gradient probe, Bruker). Reproduced from Li *et al.*³⁶ under the Attribution-NonCommercial 4.0 International Public License (CC BY-NC 4.0).

the lignin fragments and defining the structural features of the hemicellulose-derived carbohydrates in the lignin oil. The detailed characterization of the fractions by HSQC NMR measurements (Fig. 35) revealed the formation of the reduced β -O-4 linkages presenting a methylene group at the C _{α} position. It is generally accepted that stabilization processes primarily involve lignin monomer intermediates. The findings presented in this publication indicated that an additional route for the lignin stabilization has been established through the formation of the reduced β -O-4 linkages.

The next two short Sections 2.3 and 2.4 focus on the application of ³¹P, ¹⁹F, and ¹⁵N NMR to the structural studies of different types of lignin are by no means a comprehensive discussion of the subject.

2.3. ³¹P NMR

Due to the complexity of the repeating monomers in lignin, its ¹H NMR spectra suffer from significant overlap when used for

lignin analysis. However, ³¹P derivatization has been proven a useful technique for the NMR analysis of lignin. The structure of lignin can be effectively modified by the instantaneous incorporation of phosphorus into kraft lignin, so that ³¹P NMR could be applied to lignin analysis and structural studies. As an example, see paper by Puyadena *et al.*⁴⁵ on the phosphorus-containing lignin intermediates for the polyurethane and acrylic coatings for wood. The 100% natural abundance of the ³¹P isotope, the large chemical shift range, and the sharp signals provide perspectives of using ³¹P NMR for the lignin analysis.

One of the basic publications⁴⁶ of the last five years demonstrated that ³¹P NMR spectroscopy is a promising technique for the quantitative analysis of hydroxyl groups of lignin due to its unique characterization capability of the biorefinery process. The proposed protocol describes procedures for the preparation and analysis of phosphitylated lignin samples based on ³¹P NMR spectra together with the means of quantitative analysis of different types of hydroxyl groups. Compared to the traditional ‘wet-chemical techniques’, the above method of

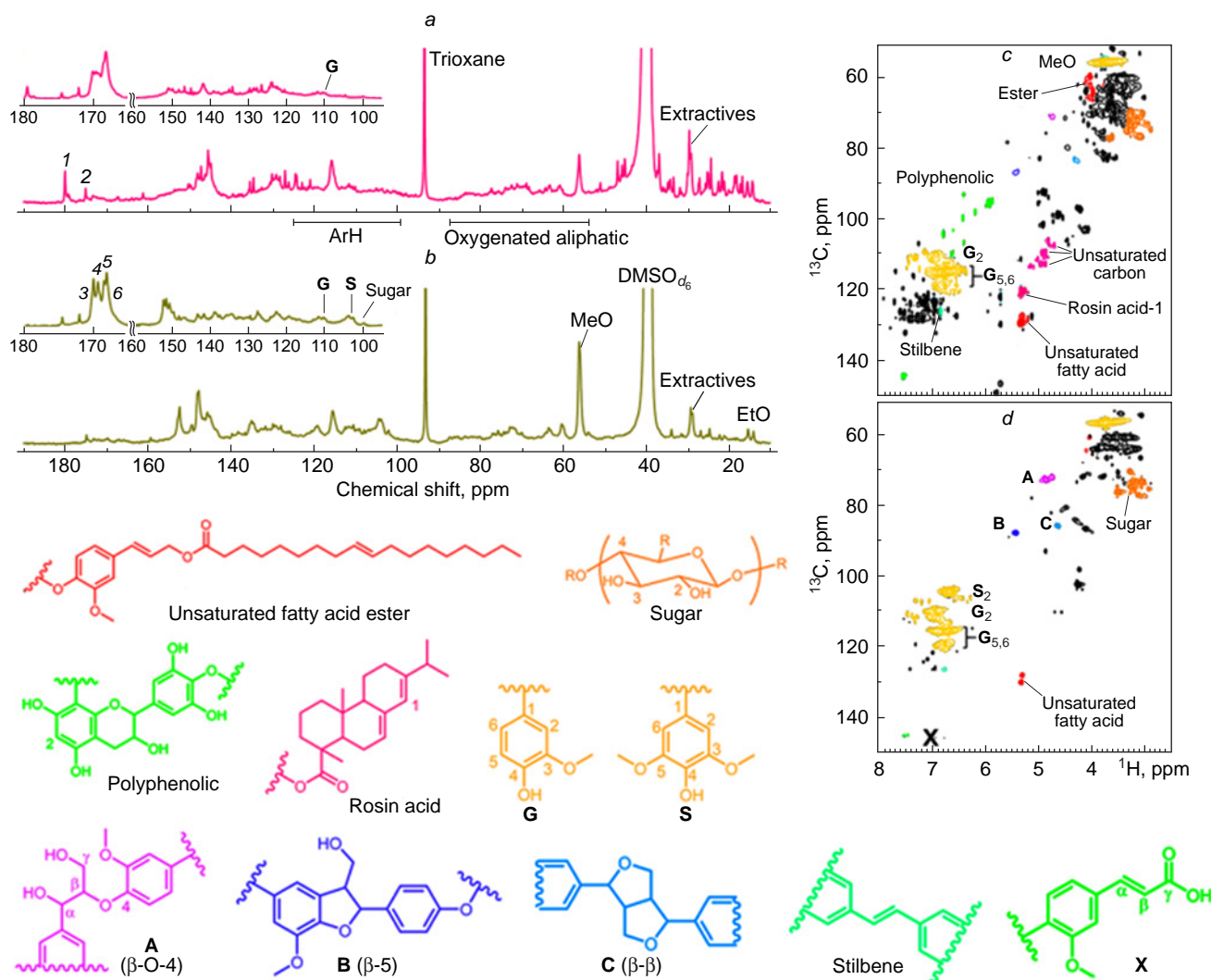


Figure 24. ^{13}C NMR spectra of organosolv crude lignin of pine bark (a), oak bark (b) and HSQC NMR spectra of organosolv crude lignin of pine bark (c), oak bark (d). The dimension of the axis in fig. a is similar to that of the axis in fig. b. ^{13}C NMR and ^1H NMR spectra were obtained on a Bruker Avance 300 MHz spectrometer at 298 K with a BBO probe. HSQC NMR spectra were obtained on a Bruker VANCE III 600 MHz spectrometer at 25°C equipped with a cryoprobe. ^{13}C NMR samples were prepared by dissolving 150–200 mg dried lignin powders or acetylated lignin powders in 450 μL $\text{DMSO-}d_6$, followed by the addition of 60 μL 50 mg mL^{-1} chromium(III) acetylacetonate as a relaxation reagent. For ^1H NMR samples, 50 mg acetylated lignin samples were dissolved in 400 μL chloroform-*d* followed by the addition of 100 μL *p*-hydroxybenzaldehyde (5 mg mL^{-1}) as an internal standard. For HSQC NMR, 30 mg dried lignin-rich compounds were dissolved in 500 μL $\text{DMSO-}d_6$. All these samples were transferred into 5 mm NMR tubes and capped. Reproduced with minor editing privileges from Liu *et al.*³⁷ with the permission of the American Chemical Society.

quantitative ^{31}P NMR spectroscopy offered unique advantages in measuring phosphorylated hydroxyl groups from a single ^{31}P NMR spectrum, as illustrated in Figures 36 and 37. In addition, this method provided complete quantitative information about hydroxyl groups in small amounts of sample (~30 mg) within a relatively short experimental time (up to 2 h).

A similar study was carried out using quantitative ^{31}P NMR of lignins and tannins from organosolv lignin, which was derivatized with TMDP.⁴⁷ Quantitative ^{31}P NMR spectroscopy was shown to be a rapid and reliable method for the identification of unsubstituted, *o*-mono-substituted and *o*-disubstituted phenols, aliphatic hydroxyls and carboxylic acids in lignins and tannins. The methodology consisted of an *in situ* quantitative ^{31}P labelling of lignin or tannin followed by the acquisition of a quantitative ^{31}P NMR spectrum (Fig. 38). However, it was concluded that TMDP-based ^{31}P NMR is unable to distinguish aryl-glycerol- β -aryl ethers, phenylcumarane and pinoresinols.

Jia *et al.*⁴⁸ determined the role of lignin produced in the autohydrolysis process in the enzymatic hydrolysis of biomass. Based on the ^{31}P NMR data, β -O-4 of lignin was reduced, while β -5 and β - β ratios increased with increasing the hydrolysis intensity. At that, the increase in the hydrolysis intensity significantly enhanced the content of condensed and non-condensed phenolic OH groups of lignin. It was also shown by ^{31}P NMR that the cellulase enzyme adsorbs more readily onto lignin with higher phenolic content, and its association with lignin reduces its activity to hydrolyze cellulose microcrystals.

Mun *et al.*⁴⁹ carried out ^{31}P NMR analysis of kraft lignin prepared from mixed hardwoods, as illustrated in Figure 39, which shows the enlarged region (134–150 ppm) of phosphorylated hydroxyl groups in syringyl, guaiacyl and *p*-hydroxyphenyl moieties. A sharp peak at 174 ppm was attributed to the excess amount of unreacted TMDP indicating that all hydroxyls in kraft lignin were completely derivatized.

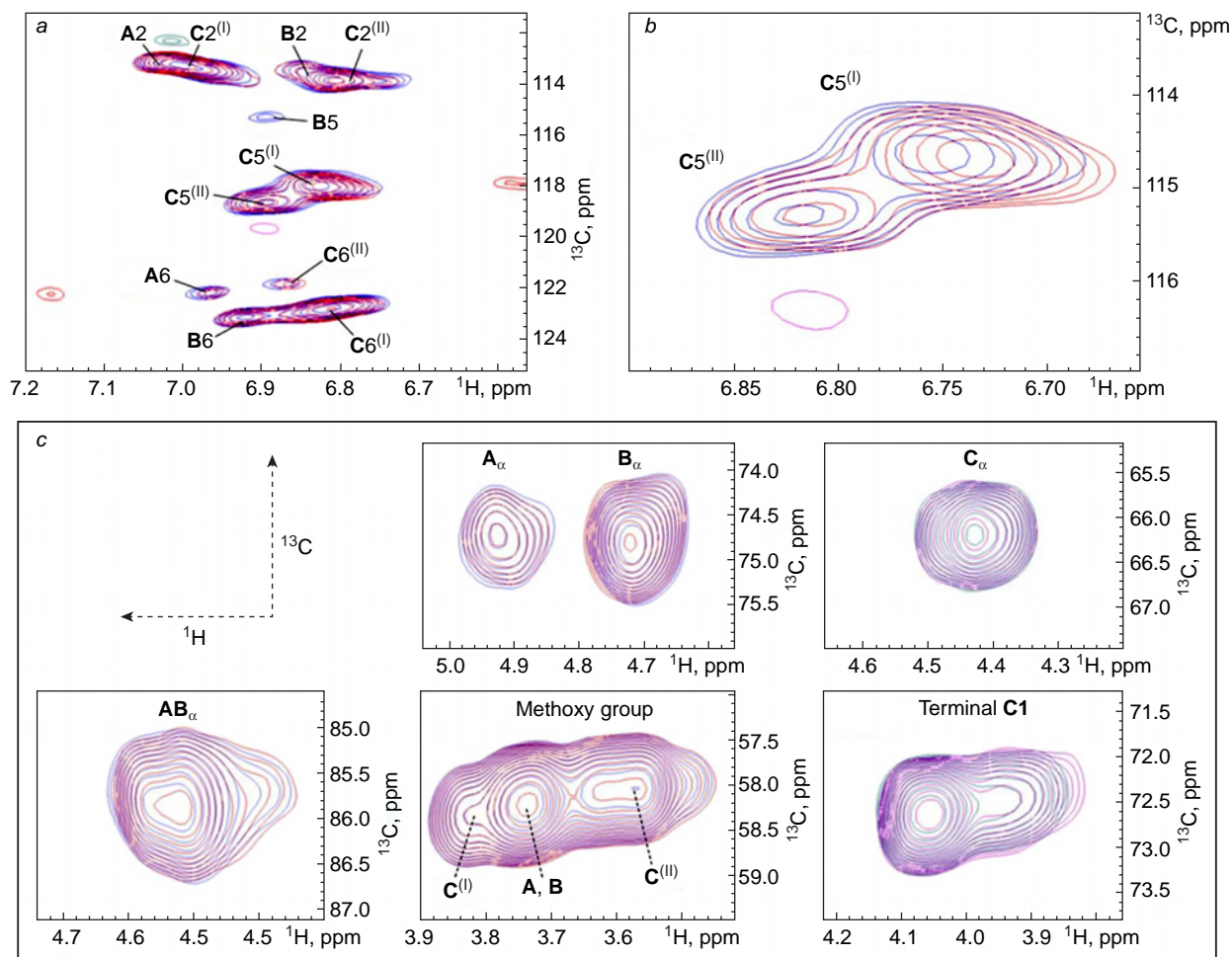


Figure 27. 2D ^1H - ^{13}C HSQC spectra of the long-chain ^{13}C -labeled lignin oligomer models in the NMR experiments. Superimposed 2D ^1H - ^{13}C HSQC spectra of the aromatic region in the presence (red) and absence (blue) of $350\ \mu\text{M}$ TrCBM_1 (a). A magnified image of the HSQC signals from the C-5 positions (b). Superimposed 2D ^1H - ^{13}C HSQC spectra of aliphatic regions and methoxy groups in the presence (red) and absence (blue) of $350\ \mu\text{M}$ TrCBM_1 (c). For used designations and abbreviations, see original text. Each sample was dissolved in 50 mM acetic acid- d_4 buffer, which was prepared using D_2O (pD 5.0) and 10% (v/v) $\text{DMSO-}d_6$. Each 250 μL NMR sample was placed in a 5-mm Shigemi symmetrical microtube (Shigemi, Japan) and contained 20 μM 2,2-dimethyl-2-silapentane-5-sulfonic acid as an internal standard. All NMR spectra were recorded on a Bruker Avance III HD 600 spectrometer equipped with a cryogenic probe and Z gradient (Bruker BioSpin, USA). Reproduced with minor editing privileges from Tokunaga *et al.*³⁹ under the Attribution-NonCommercial 4.0 International Public License (CC BY-NC 4.0).

may arise from the wide range of lignosulfonates from different wood sources, pulping conditions, and purification procedures used in biorefineries. Finding a suitable solvent system is even more difficult for chemically modified or fractionated lignosulfonates. Wurzer *et al.*⁵² proposed a novel and fast approach for the solubilization of genuine, modified, and fractionated lignosulfonates and subsequent quantitative analysis of hydroxy groups by ^{31}P NMR after derivatization with TMDP.

Another application that deserves to be cited is the successful utilization of ^{31}P NMR for studying the oxidation of kraft lignin in view of preparing lignin vitrimers, which are currently frontier materials in lignin chemistry. It is well known that the valorization of lignin into the commercial products by oxidative conversion is a widely studied strategy. However, in many cases, this approach has limited scope for integration into industrial processes.

In general, ^{31}P NMR spectroscopy is used for either the qualitative or the quantitative determination of hydroxylated

moieties as well as for determination of the condensation degree and the syringyl/guaiacyl ratio in lignins.

Of some practical interest is somehow also the benchtop NMR spectroscopy, which is used for the low-cost analytical analysis of lignin (Fig. 41). The benchtop NMR instrumentation offers the possibility to measure ^{31}P NMR spectra in situations where the application of the high-field NMR spectroscopy is unavailable or too expensive. The former technique provides the ability to quantify different classes of compounds less accurately but at lower cost. Further examples of the benchtop NMR investigations of different lignins (like kraft softwood and hardwood lignins, organosolv hardwood lignin, and soda lignin) have been reported by Araneda *et al.*⁵³

2.4. NMR of other nuclei

Examples of this type are very rare because NMR of other nuclei such as ^{15}N or ^{19}F requires isotopic labelling and/or chemical modification of lignin, which is rather expensive and/or time-consuming.

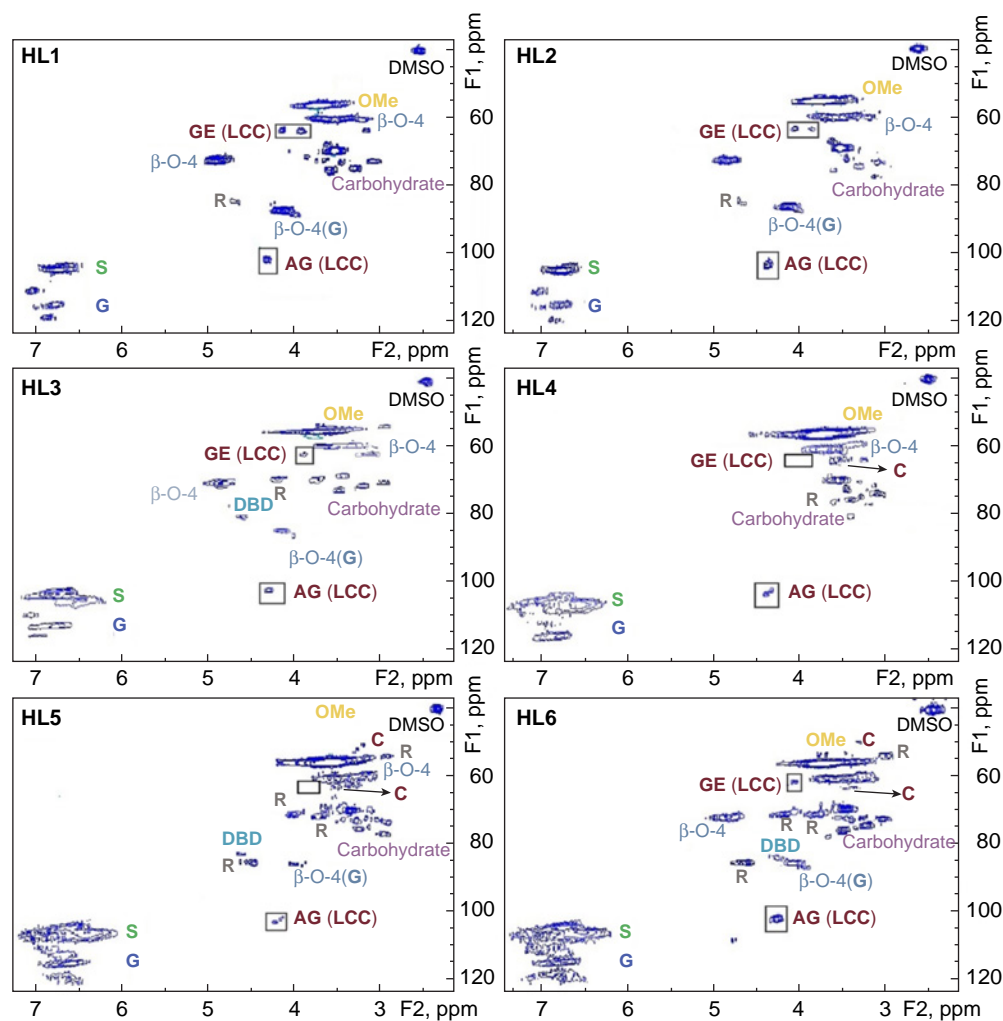


Figure 28. 2D HSQC spectra of six hydrolyzed lignin samples (HL1–HL6). The identified cross peaks are: β -O-4 aryl ether (β -O-4); β -O-4 aryl ether in guaiacyl β -O-4 (G); γ -ester GE (LCC); glycoside PG (LCC); methoxy group (OMe); syringyl (S); guaiacyl (G); Phenylcoumaran (β -5) (C); dibenzodioxcin (5-5-O-4) (DBD); resinol (R). For used designations and abbreviations, see original publication. The ^1H – ^{13}C HSQC spectra were recorded on a 500 MHz Bruker Avance NEO spectrometer equipped with a 5 mm Quattro Nucleus Probe and a field gradient. For the NMR experiments, 50 mg of the hydrolyzed lignin samples were added to 0.7 mL of $\text{DMSO-}d_6$ and stirred at 45°C overnight. Reproduced with minor editing privileges from Ghavidel *et al.*⁴⁰ with the permission of Elsevier.

One of those rare examples appeared during the last 5 years, is the NMR study of the molecular interaction of lignin with amino acid residues of the ^{15}N -labelled carbohydrate-binding module.⁵⁴ The authors reported NMR-based analyses of the binding sites of a carbohydrate-binding module of cellobiohydrolase 1 from a hypercellulase-producing fungus. A unique method was developed to obtain *Trichoderma reesei* carbohydrate-binding module 1 at the C-terminal domain (*Tr*-CBM1). Chemical shift analysis revealed that *Tr*-CBM1 was adsorbed onto cellohexaose in a highly specific manner *via* two subsites, the flat plane surface and the cleft, which were located on the opposite sides of the protein surface. Spectral assignments of $^{13}\text{C}/^{15}\text{N}$ -labelled *Tr*-CBM1 were performed by a standard sequential assignment procedure. As an illustrative example, the ^1H – ^{15}N HSQC spectrum of ^{15}N -labelled *Tr*-CBM1 is shown in Figure 42. The final backbone assignments of *Tr*-CBM1 were unambiguously made by the authors, however with the exception of eight residues.

The second example deals with the ^{19}F NMR study of the phenolic hydroxyl groups in lignin modified by pentafluoropyridine, as was reported in 2023 by Kenny *et al.*⁵¹ The authors proposed a complementary method based on ^{19}F NMR spectroscopy that enabled accurate identification and quantification of phenolic groups in lignin samples by using pentafluoropyridine as a derivatizing reagent. The ^{19}F NMR spectrum of the resulting tetrafluoropyridine ether (Fig. 43) showed signals of two sets of identical fluorine atoms, which gave rise to resonances in two distinct regions, namely a

downfield (designated as ‘DF’ in Fig. 43) region, from –89 to –95 ppm (fluorine atoms and integration region are marked blue), and an upfield (designated as ‘UF’ in Fig. 43) region, from –155 to –162 ppm (fluorine atoms and integration region are marked red).

However, the use of ^{19}F NMR spectroscopy is still under revision and it is not at the level of ^{31}P NMR for the quantitative and qualitative analyses of hydroxylated moieties of lignins. The former technique is especially suitable for the lignin-derived products such as pyrolysis oils.

3. Conclusion

Recent applications of the one- and two-dimensional ^1H and ^{13}C NMR spectroscopy together with NMR of less popular nuclei such as ^{31}P , ^{19}F and ^{15}N to the structural studies of lignin and lignin-derived products in liquid phase have provided a solid breakthrough and a practical guide to their molecular organization. In this respect, ^1H and ^{13}C one-dimensional NMR spectra together with different modifications of two-dimensional ^1H – ^{13}C HSQC pulse sequences should first be mentioned. Also, NMR of less popular nuclei such as ^{31}P , ^{19}F , and ^{15}N are of considerable interest and are a guiding thread in the structural studies of lignin.

Quantitative NMR spectra of ^1H and ^{13}C together with less popular nuclei such as ^{31}P , ^{19}F , and ^{15}N are extensively used to characterize different structural units of lignin (syringyl, oxidized syringyl, guaiacyl, *p*-hydroxyphenyl, ferulic acid,

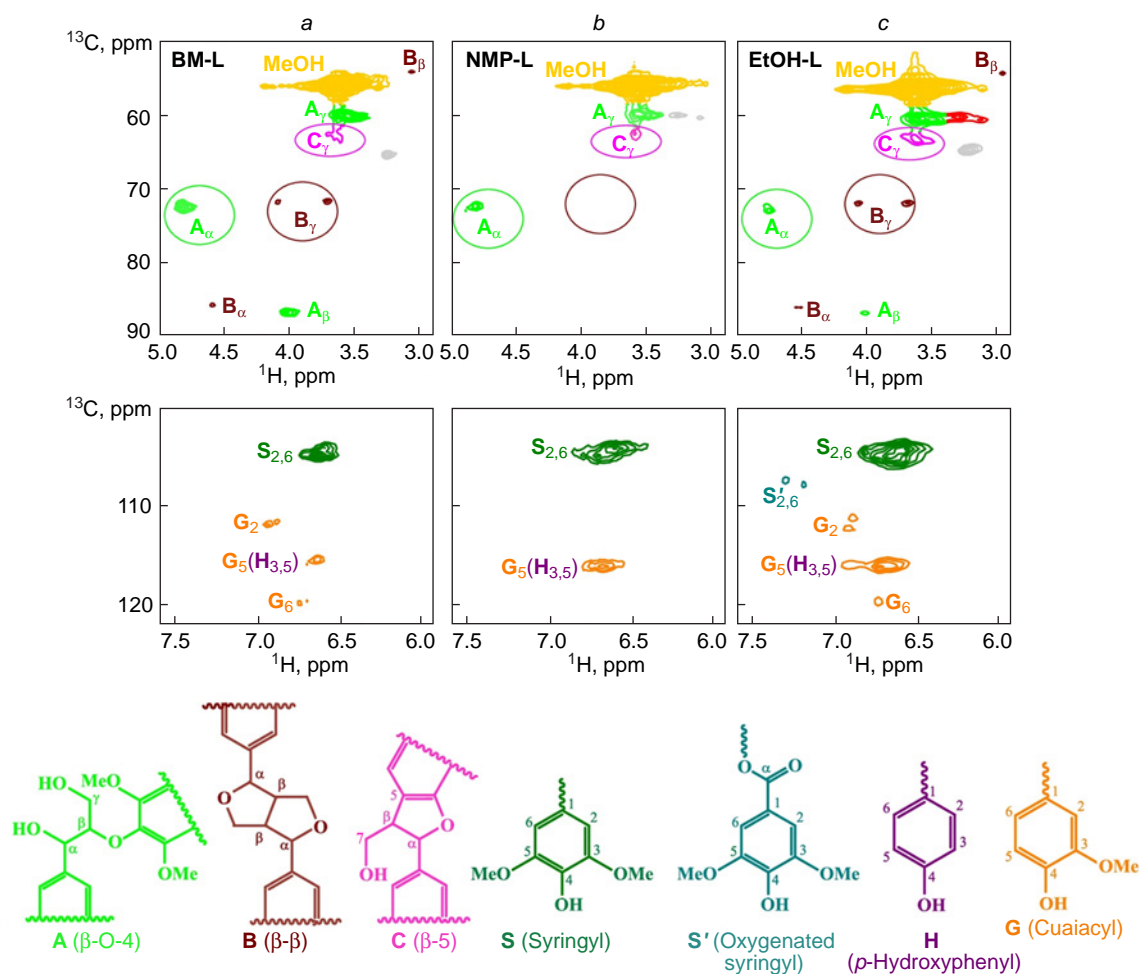


Figure 29. 2D HSQC spectra of the side-chain and aromatic regions of the ball milled lignin (**BM-L**) (a), NMP-pretreated lignin (b) and ethanol lignin from *Acacia confuse* wood (c). All 2D-HSQC ^1H - ^{13}C experiments were performed on a 500-MHz spectrometer JEOL ECZR equipped with a 5-mm probe. A standard pulse sequence was applied with the following parameters: spectral widths of 11 ppm in F2 (^1H) with 1024 data points and 190 ppm in F1 (^{13}C) with 256 data points, 64 scans, and 1.5 seconds interscan delay. For each test, 50 mg of purified lignin sample was dissolved in 0.5 ml of $\text{DMSO-}d_6$. Reproduced from Islam *et al.*⁴¹ with the permission of Springer Nature.

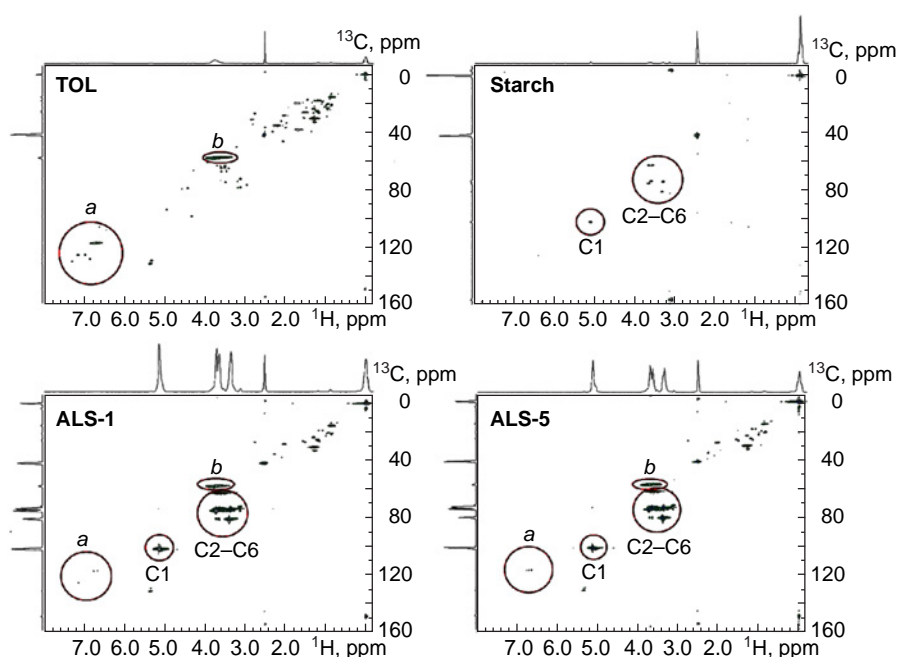


Figure 30. The ^1H - ^{13}C HSQC spectra of tall oil lignin (**TOL**), starch and anionic tall oil lignin-starch copolymers (**ALS-1** and **ALS-5**). Red circles indicate the corresponding cross-peaks of the aromatic region and methoxy groups. For details, see original publication. All ^1H - ^{13}C 2D-HSQC experiments were performed on a Varian UNITY INOVATM-500 MHz NMR spectrometer using 26–27 mg of previously dried samples in 500 μL of $\text{DMSO-}d_6$. Reproduced with minor editing privileges from Diaz-Baca *et al.*⁴² with the permission of the American Chemical Society.

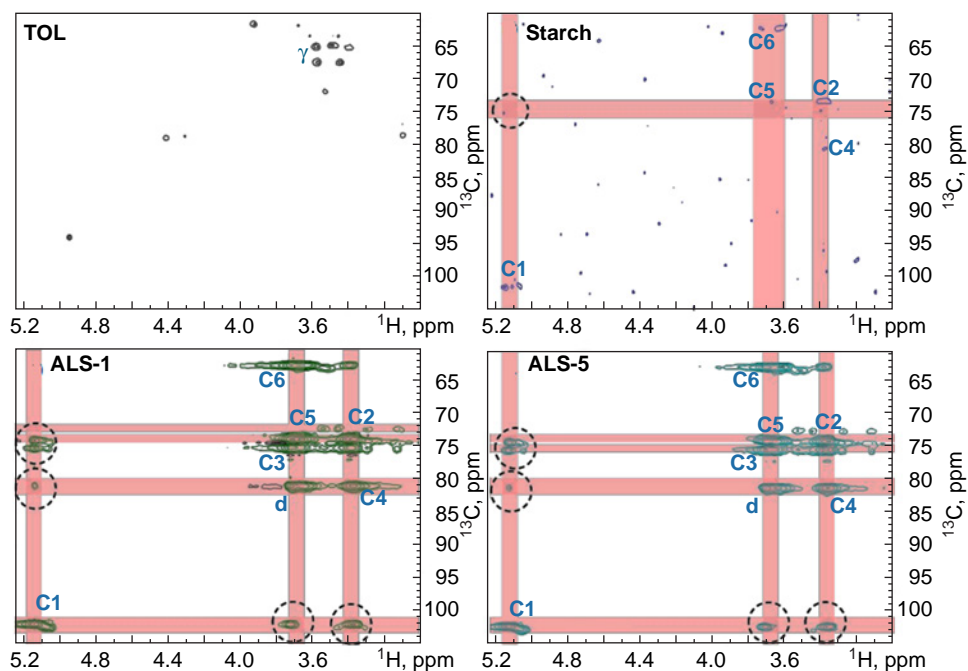


Figure 31. The ^1H - ^{13}C HSQC-TOCSY spectra of tall oil lignin (TOL), starch, and anionic tall oil lignin-starch copolymers, ALS-1 and ALS-5. Dotted circles indicate TOCSY correlations of carbons (vertical) and protons (horizontal). For details, see original publication. All ^1H - ^{13}C 2D-HSQC experiments were performed on a Varian UNITY INOVATM-500 MHz NMR spectrometer using 26–27 mg of previously dried samples in 500 μL of $\text{DMSO-}d_6$. Reproduced with minor editing privileges from Diaz-Baca *et al.*⁴² with the permission of the American Chemical Society.

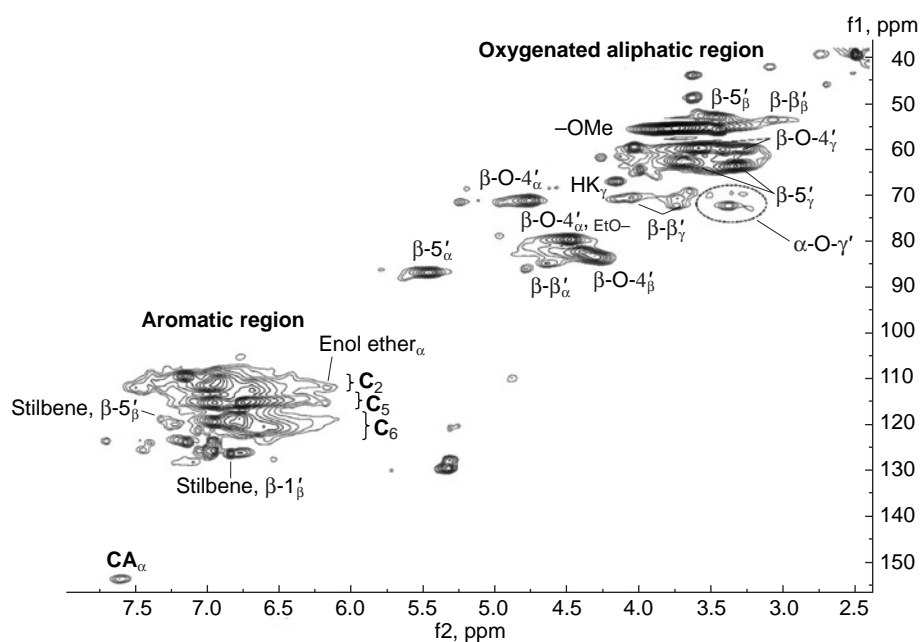


Figure 32. 2D ^1H - ^{13}C HSQC NMR spectrum of the ethanol-soluble portion of the extracted lignin sample; f1 corresponds to the ^{13}C dimension and f2 — to the ^1H dimension. The NMR spectra were recorded in $\text{DMSO-}d_6$ on a Bruker NMR spectrometer Avance III HD 400 MHz instrument (Bruker Corporation, USA) equipped with a 5 mm Z-gradient BBFO broadband smart probe. Reproduced from Karlsson *et al.*⁴³ under the Attribution-Non-Commercial 4.0 International Public License (CC BY-NC 4.0).

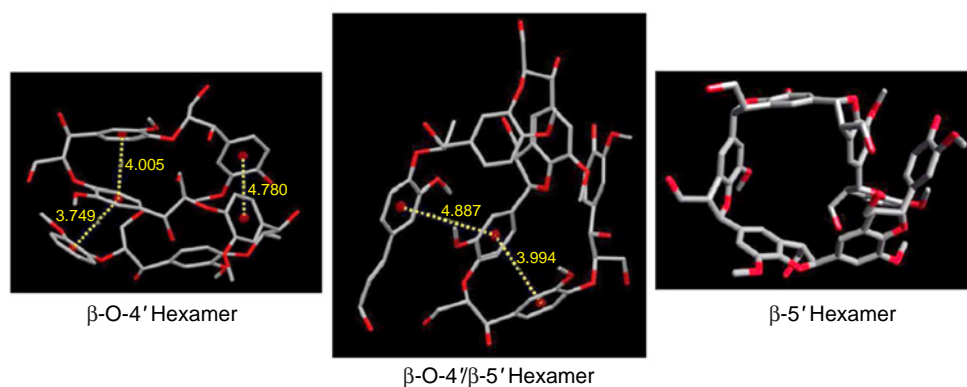


Figure 33. DFT models of three hexamers. Yellow dotted lines indicate the π - π stacked aromatic rings for both sandwich and the T-shape type stacking. Reproduced with minor editing privileges from Karlsson *et al.*⁴³ under the Attribution-Non-Commercial 4.0 International Public License (CC BY-NC 4.0).

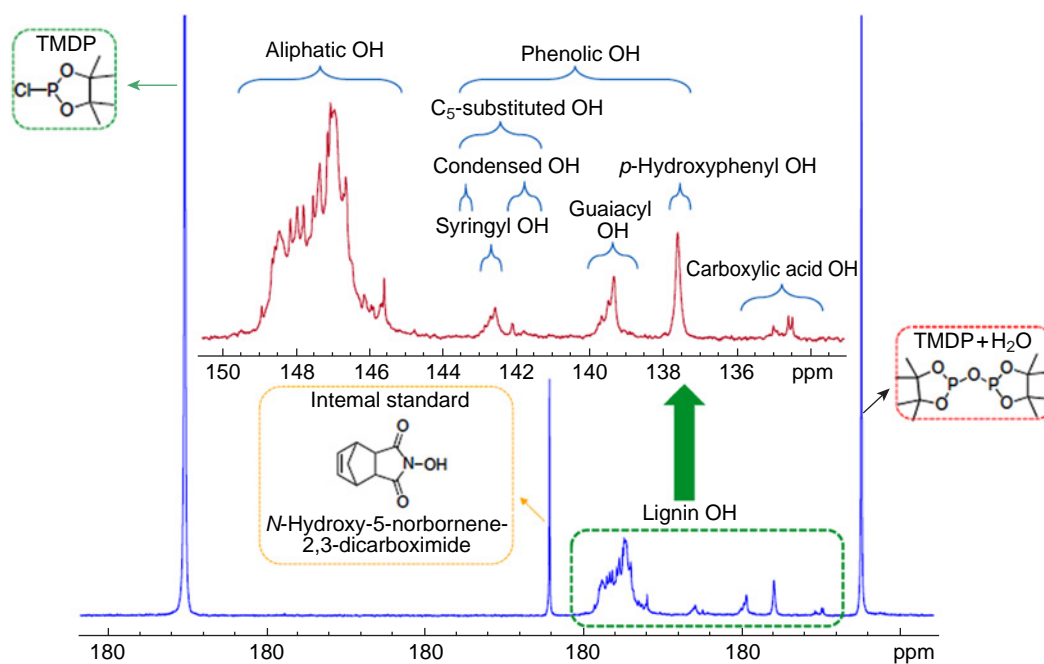


Figure 36. A quantitative ^{31}P NMR spectrum of a hardwood poplar lignin derivatized with 1-chloro-4,4',5,5'-tetramethyl-1,3-dioxane-2-phospholane (TMDP). All spectra were recorded on a Bruker Avance III HD 500-MHz spectrometer equipped with a 5-mm BBO probe in $\text{DMSO-}d_6$. Reproduced from Meng *et al.*⁴⁶ under the Attribution-NonCommercial 4.0 International Public License (CC BY-NC 4.0).

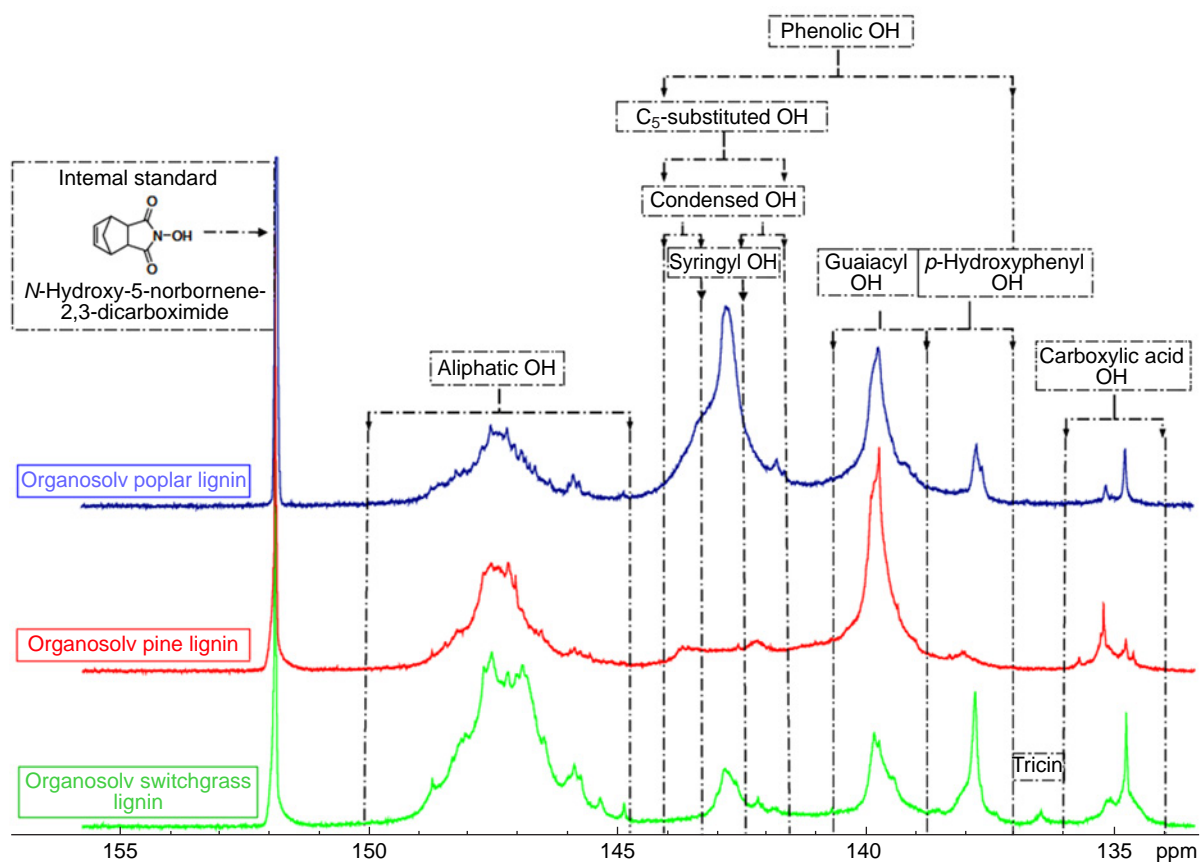


Figure 37. Quantitative ^{31}P NMR spectra of organosolv poplar, pine, and switchgrass lignins derivatized with TMDP. All spectra were recorded on a Bruker Avance III HD 500-MHz spectrometer equipped with a 5-mm BBO probe in $\text{DMSO-}d_6$. Reproduced from Meng *et al.*⁴⁶ under the Attribution-NonCommercial 4.0 International Public License (CC BY-NC 4.0).

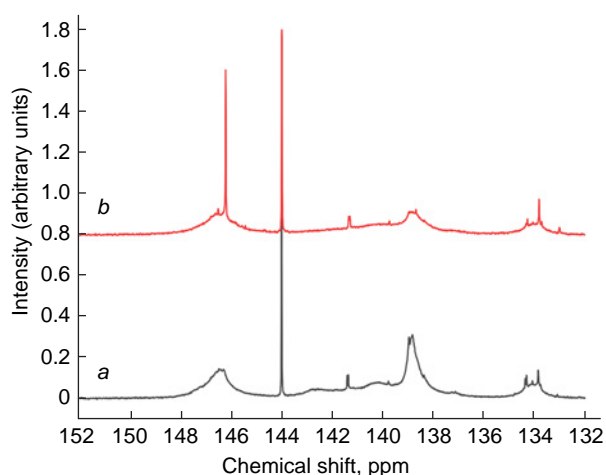


Figure 38. Quantitative ^{31}P NMR spectra of organosolv lignin derivatized with TMDP before (a) and after oxidation (b). The spectra were recorded on a 300 MHz NMR spectrometer in pyridine/deuterated chloroform. Reproduced from Argyropoulos *et al.*⁴⁷ under the Attribution-NonCommercial 4.0 International Public License (CC BY-NC 4.0).

spectroscopy over the last few decades and especially the last five years have revealed characteristic functional groups of lignin and lignin-related products together with the spectral regions in which they resonate. These data provide a straightforward insight into the chemical structure and stereochemistry of different lignins.

4. List of abbreviations

- Ac-KL — acetylated kraft lignin,
- Ac-MWL — acetylated milled wood lignins,
- Ac-MWL-aca — acetylated milled wood lignins from acacia,
- Ac-MWL-mhw — acetylated milled wood lignins from mixed hardwood,
- APTAC — (3-acrylamidopropyl) trimethyl ammonium chloride,
- BL — bioenzymatic lignin,
- COSY — COrelated SpectroscopY,
- Cu-AHP — Cu-catalyzed alkaline hydrogen peroxide lignin,
- DF — downfield,
- DFT — density functional theory,
- DSS — 2,2-dimethyl-2-silapentane-5-sulfonic acid,

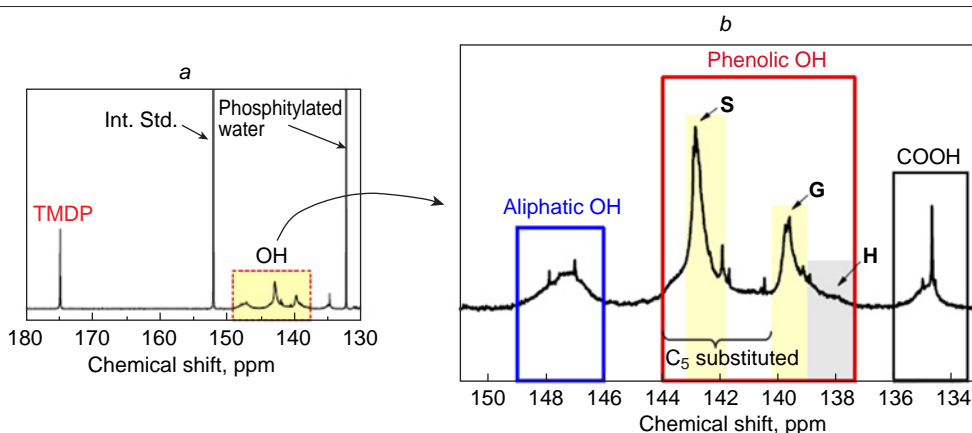


Figure 39. ^{31}P NMR spectrum of kraft lignin prepared from mixed hardwoods showing phosphitylated hydroxyl groups in syringyl (S), guaiacyl (G) and *p*-hydroxyphenyl (H) moieties. Spectra were recorded on a 500 MHz spectrometer (Jeol, Japan) in pyridine/deuterated chloroform. Reproduced from Mun *et al.*⁴⁹ under the Attribution-NonCommercial 4.0 International Public License (CC BY-NC 4.0).

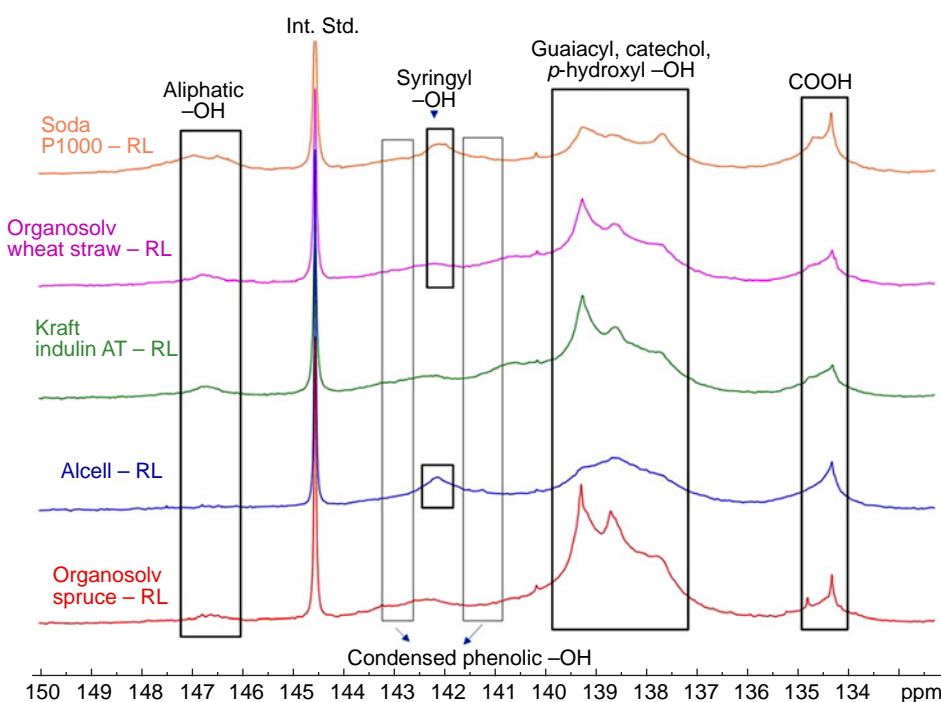


Figure 40. ^{31}P NMR spectrum of various lignin residues (RL) obtained after base-catalyzed depolymerization (after phosphitylation). All spectra were recorded on a Bruker AVANCE III 400 MHz instrument in DMSO- d_6 using a standard phosphorous pulse programmer. Reproduced from Purushothaman *et al.*⁵⁰ under the Attribution-NonCommercial 4.0 International Public License (CC BY-NC 4.0).

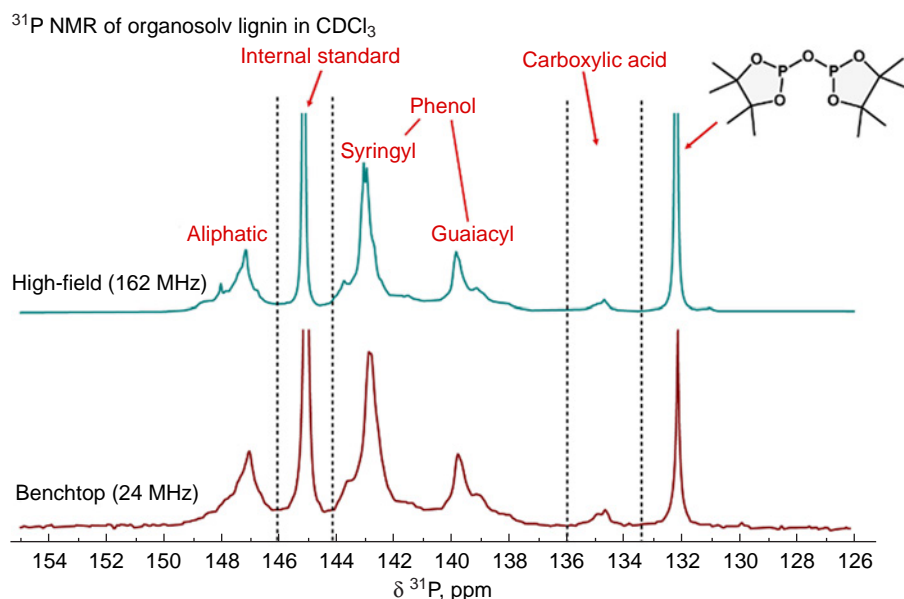


Figure 41. Highfield and benchtop ^{31}P NMR spectra of phosphitylated lignin. All benchtop ^{31}P NMR spectra were obtained on a Nanalysis 60pro benchtop NMR spectrometer operating at 24.3 MHz ^{31}P frequency. All high-field ^{31}P NMR spectra were obtained on a Bruker 400 MHz Avance III spectrometer operating at 162 MHz ^{31}P frequency. Reproduced from <https://cdsciencepub.com/doi/full/10.1139/cjc-2022-0041> under the Attribution-NonCommercial 4.0 International Public License (CC BY-NC 4.0).

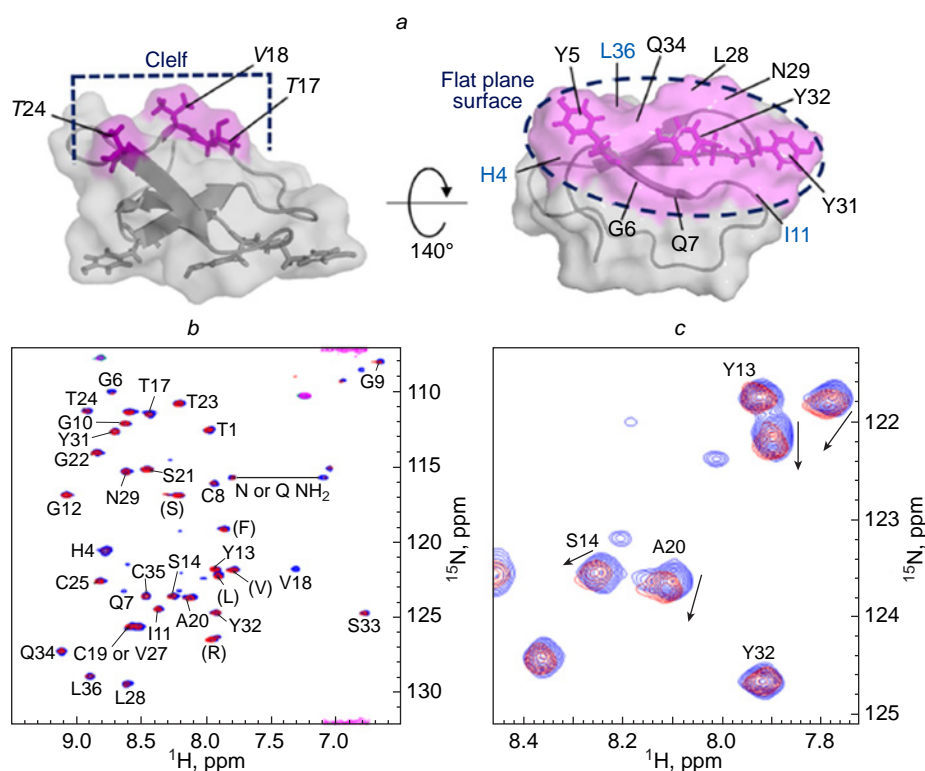


Figure 42. Proposed structure of *TrCBM1* (a); 2D ^1H - ^{15}N HMBC spectra of NMR titration experiments using ^{15}N -labelled *TrCBM1* (b); (c) the close-up view of the region exhibited fairly large perturbations (c). For details, see original publication. NMR spectra were recorded on a Bruker Avance III 600 spectrometer equipped with a cryogenic probe and Z-gradient (Bruker BioSpin, USA). For NMR experiments, 150 μM of the $^{13}\text{C}/^{15}\text{N}$ -labeled *TrCBM1* was dissolved in 45 mM sodium acetate buffer (pH 5.0), containing 10% D_2O and 20 μM 2,2-dimethyl-2-silapentane-5-sulfonic acid (DSS). Reproduced with minor editing privileges from Tokunaga *et al.*⁵⁴ under the Attribution-NonCommercial 4.0 International Public License (CC BY-NC 4.0).

G — guaiacyl,
H — *p*-hydroxyphenyl,
HL — hydrolyzed lignin,
HMBC — heteronuclear multiple bond correlation,
HSQC — heteronuclear single quantum coherence,
HSQC-TOCSY — Heteronuclear Single Quantum Coherence in combination with Total Correlation Spectroscopy,
HSQC₀ — heteronuclear single-quantum coherence zero,
Int. Std. — internal standard,
KL — kraft lignin,
MWL — milled wood lignin,
OL — organosolv lignin,
*p*BA — *p*-hydroxybenzoates,
*p*CA — *p*-coumarates,
S — syringyl,

SBL — sulfobutylated lignin,
SML — sulfomethylated lignin,
TMDP — 1-chloro-4,4',5,5'-tetramethyl-1,3-dioxo-2-phospholane,
TOL — Tall Oil Lignin,
*TrCBM*₁ — *Trichoderma reesei* carbohydrate-binding module 1,
UF — upfield.

5. References

1. E.I.Evstigneyev, D.N.Zakusilo, D.S.Ryabukhin, A.V.Vasilyev. *Russ. Chem. Rev.*, **92**, RCR5082 (2023); <https://doi.org/10.59761/RCR5082>

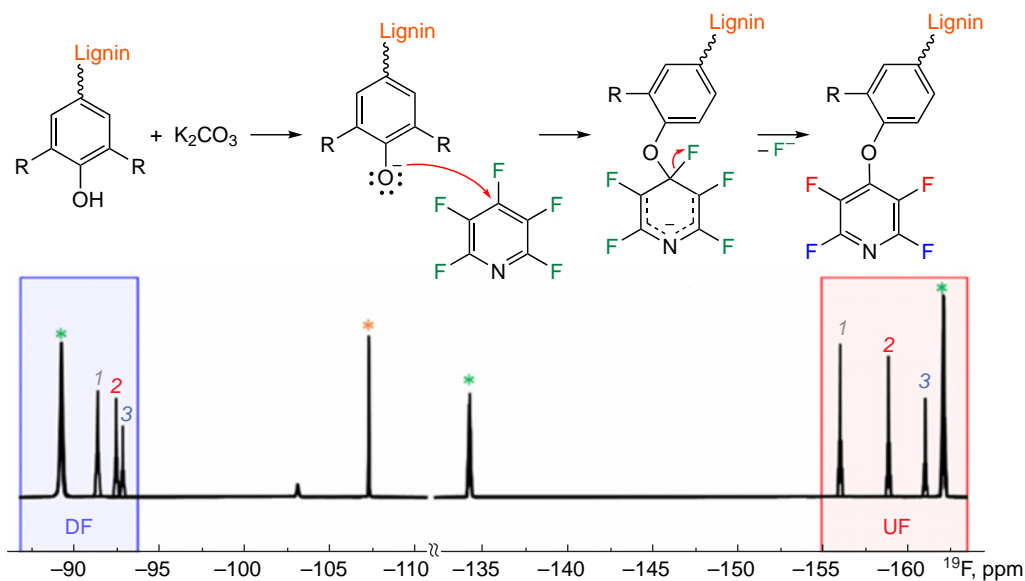


Figure 43. ^{19}F NMR spectrum of the reaction of pentafluoropyridine with a phenolic compound to form a tetrafluoropyridine ether. Resonances marked with a green asterisk belong to pentafluoropyridine, and the resonance marked with an orange asterisk relates for the internal standard, 4,4-difluorobenzophenone. Numbered resonances correspond to 4-propylphenol (1), 4-propylguaiacol (2) and 4-propylsyringol (3), respectively. Reproduced with minor editing privileges from Kenny *et al.*⁵¹ under the Attribution-Non-Commercial 4.0 International Public License (CC BY-NC 4.0).

- M. Balakshin, E.A. Capanema, X. Zhu, I. Sulaeva, A. Potthast, T. Rosenau, O.J. Rojas. *Green Chem.*, **22**, 3985 (2020); <https://doi.org/10.1039/D0GC00926A>
- J. Ralph, L.L. Landucci. In *Lignin and Lignans: Advances in Chemistry. NMR of Lignins*. (Eds C. Heitner, D.R. Dimmel, J.A. Schmidt). (Boca Raton, London: CRC Press, 2010)
- K. Lundquist. In *Methods in Lignin Chemistry. Springer Series in Wood Science*. (Eds S.Y. Lin, C.W. Dence). (London: Springer-Verlag, 1992). P. 242
- D. Robert. In *Methods in Lignin Chemistry. Springer Series in Wood Science*. (Eds S.Y. Lin, C.W. Dence). (London: Springer-Verlag, 1992). P. 250
- S. Li, K. Lundquist. *Nord. Pulp Paper Res. J.*, **9**, 191 (1994); <https://doi.org/10.3183/npprj-1994-09-03-p191-195>
- B.B. Hallac, Y. Pu, A.J. Ragauskas. *Energy Fuels*, **24**, 2723 (2010); <https://doi.org/10.1021/ef901556u>
- M. Sette, R. Wechselberger, C. Crestini. *Chem. – Eur. J.*, **17**, 9529 (2011); <https://doi.org/10.1002/chem.201003045>
- M. Sette, H. Lange, C. Crestini. *Comp. Struct. Biotechnol. J.*, **6**, e201303016 (2013); <https://doi.org/10.5936/csbj.201303016>
- Yu. Archipov, D.S. Argyropoulos, H.I. Bolker, C. Heitner. *J. Wood Chem. Technol.*, **11**, 137 (1991); <https://doi.org/10.1080/02773819108050267>
- M.T. Amiri, S. Bertella, Y.M. Questell-Santiago, J.S. Luterbacher. *Chem. Sci.*, **10**, 8135 (2019); <https://doi.org/10.1039/C9SC02088H>
- C.L. Bourmaud, S. Bertella, A.B. Rico, S.D. Karlen, J. Ralph, J.S. Luterbacher. *Angew. Chem., Int. Ed.*, **63**, e202404442 (2024); <https://doi.org/10.1002/anie.202404442>
- L.B. Krivdin. *Magn. Reson. Chem.*, **57**, 897 (2019); <https://doi.org/10.1002/mrc.4873>
- L.B. Krivdin. *Magn. Reson. Chem.*, **58**, 5 (2020); <https://doi.org/10.1002/mrc.4896>
- L.B. Krivdin. *Magn. Reson. Chem.*, **58**, 15 (2020); <https://doi.org/10.1002/mrc.4895>
- L.B. Krivdin. *Prog. NMR Spectrosc.*, **108**, 17 (2018); <https://doi.org/10.1016/j.pnmrs.2018.10.002>
- L.B. Krivdin. *Prog. NMR Spectrosc.*, **112–113**, 103 (2019); <https://doi.org/10.1016/j.pnmrs.2019.05.004>
- L.B. Krivdin. *Prog. NMR Spectrosc.*, **102–103**, 98 (2017); <https://dx.doi.org/10.1016/j.pnmrs.2017.08.001>
- V.A. Semenov, L.B. Krivdin. *Russ. Chem. Rev.*, **91** (5), RCR5027 (2022); <https://doi.org/10.1070/RCR5027?locatt=label:RUSSIAN>
- L.B. Krivdin. *Molecules*, **26**, 2450 (2021); <https://doi.org/10.3390/molecules26092450>
- L.B. Krivdin. *Magn. Reson. Chem.*, **58**, 478 (2020); <https://doi.org/10.1002/mrc.4965>
- L.B. Krivdin. *Magn. Reson. Chem.*, **58**, 500 (2020); <https://doi.org/10.1002/mrc.4973>
- A.V. Levdansky, A.A. Kondrasenko, Yu.N. Malyara, V.A. Levdanskaya, B.N. Kuznetsov. *J. Siber. Fed. Univ.*, **12**, 201 (2019)
- D. Ye. Hopa, P. Fatehi. *Polymers*, **12**, 2046 (2020); <https://doi.org/10.3390/polym12092046>
- L. Zhao, J. Diaz-Baca, A. Salaghi, J. Gao, Y. Wang, Q. Wang, P. Fatehi. *Ind. Crops Prod.*, **202**, 117069 (2023); <https://doi.org/10.1016/j.indcrop.2023.117069>
- X. Wang, W. Gao, B. Liao, P. Fatehi. *ACS Omega*, **8**, 27156 (2023); <https://doi.org/10.1021/acsomega.3c02296>
- J.-S. Mun, J.A. Pe III, S.-P. Mun. *Molecules*, **26**, 4861 (2021); <https://doi.org/10.3390/molecules26164861>
- J. Rönnols, E. Danieli, H. Freichels, F. Aldaeus. *Holzforchung*, **74**, 226 (2020); <https://doi.org/10.1515/hf-2018-0282>
- Y. Li, B. Demir, L.M.V. Ramos, M. Chen, J.A. Dumesic, J. Ralph. *Green Chem.*, **21**, 3561 (2019); <https://doi.org/10.1039/c9gc00986h>
- X. Liu, Y. Li, C.M. Ewulonu, J. Ralph, F. Xu, Q. Zhang, M. Wu, Y. Huang. *ACS Sustainable Chem. Eng.*, **7**, 14135 (2019); <https://doi.org/10.1021/acssuschemeng.9b02800>
- H. Wang, B. Wang, D. Sun, Q. Shi, L. Zheng, S. Wang, S. Liu, R. Xia, R. Sun. *ChemSusChem*, **12**, 1059 (2019); <https://doi.org/10.1002/cssc.201802592>
- C. Zhao, J. Huang, L. Yang, F. Yue, F. Lu. *Ind. Eng. Chem. Res.*, **58**, 5707 (2019); <https://doi.org/10.1021/acs.iecr.9b00499>
- Y. Cao, S.S. Chen, D.C.W. Tsang, J.H. Clark, V.L. Budarin, C. Hu, K.C.-W. Wu, S. Zhang. *Green Chem.*, **22**, 725 (2020); <https://doi.org/10.1039/c9gc03553b>
- X. Chen, K. Zhang, L.-P. Xiao, R.-C. Sun, G. Song. *Biotechnol. Biofuels*, **13**, 2 (2020); <https://doi.org/10.1186/s13068-019-1644-z>
- H. Kim, Q. Li, S.D. Karlen, R.A. Smith, R. Shi, J. Liu, C. Yang, S. Tunlaya-Anukit, J.P. Wang, H.-M. Chang, R.R. Sederoff, J. Ralph, V.L. Chiang. *ACS Sustainable Chem. Eng.*, **8**, 3644 (2020); <https://dx.doi.org/10.1021/acssuschemeng.9b06389>
- Q. Li, C. Hu, M. Li, P. Truong, M.T. Naik, D. Prabhu, L. Hoffmann Jr., W.L. Rooney, J.S. Yuan. *iScience*, **23**, 101405 (2020); <https://doi.org/10.1016/j.isci.2020.101405>
- L.-Y. Liu, S.C. Patankar, R.P. Chandra, N. Sathitsuksanoh, J.N. Saddler, S. Rennecker. *ACS Sustainable Chem. Eng.*, **8**, 4745 (2020); <https://dx.doi.org/10.1021/acssuschemeng.9b06692>

38. J.L.Rowlandson, T.J.Woodman, S.R.Tennison, K.J.Edler, V.Ting. *Waste Biomass Valoriz.*, **11**, 2863 (2020); <https://doi.org/10.1007/s12649-018-0537-x>
39. Y.Tokunaga, T.Nagata, K.Kondo, M.Katahira, T.Watanabe. *Biotechnol. Biofuels*, **13**, 164 (2020); <https://doi.org/10.1186/s13068-020-01805-w>
40. N.Ghavidel, M.K.R.Konduri, P.Fatehi. *Ind. Crops Prod.*, **172**, 113950 (2021); <https://doi.org/10.1016/j.indcrop.2021.113950>
41. M.K.Islam, J.Guan, S.Rehman, R.D.Patria, C.Hu, L.Guan, S.-Y.Leu, A.K.Vuppalladiyam. *Biomass Conv. Bioref.*, **14**, 5435 (2022); <https://doi.org/10.1007/s13399-022-02655-2>
42. J.A.Diaz-Baca, A.Salaghi, P.Fatehi. *Biomacromolecules*, **24**, 1400 (2023); <https://doi.org/10.1021/acs.biomac.2c01437>
43. M.Karlsson, J.Romson, T.Elder, E.Emmer, M.Lawoko. *Biomacromolecules*, **24**, 2314 (2023)
44. R.Rinken, D.Posthuma, R.Rinaldi. *ChemSusChem*, **16**, e202201875 (2023); <https://doi.org/10.1002/cssc.202201875>
45. M.Puyadena, P.Widsten, T.Wirtanen, M.Kellock, G.Ortega, A.Mugica, E.Matxinandiarena, I.Etxeberria, L.Martin, A.Agirre, A.Barrio, A.González, L.Irusta. *Ind. Crops Prod.*, **2020**, 119261 (2024); <https://doi.org/10.1016/j.indcrop.2024.119261>
46. X.Meng, C.Crestini, H.Ben, N.Hao, Y.Pu, A.J.Ragauskas, D.S.Argyropoulos. *Nat. Protoc.*, **14**, 2627 (2019); <https://doi.org/10.1038/s41596-019-0191-1>
47. D.S.Argyropoulos, N.Pajer, C.Crestini. *J. Vis. Exp.*, **174**, e62696 (2021); <https://doi.org/10.3791/62696>
48. W.Jia, H.Shi, X.Sheng, Y.Guo, P.Fatehi, M.Niu. *Bioresour. Technol.*, **350**, 126941 (2022); <https://doi.org/10.1016/j.biortech.2022.126941>
49. J.-S.Mun, J.A.Pe III, S.-P.Mun. *BioResources*, **17**, 6626 (2022); <https://doi.org/10.15376/biores.17.4.6626-6637>
50. R. K.P.Purushothaman, G.van Erven, D.S.van Es, L.Rohrbach, A.E.Frissen, J.van Haveren, R.J.A.Gosselink. *RSC Adv.*, **13**, 4898 (2023); <https://doi.org/10.1039/d2ra06998a>
51. J.Kenny, J.Medlin, G.Beckham. *ACS Sustainable Chem. Eng.*, **11**, 5644 (2023); <https://doi.org/10.1021/acssuschemeng.3c00115>
52. G.K.Wurzer, M.Bacher, H.Hettegger, I.Sumerskii, O.Musl, K.Fackler, R.H.Bischof, A.Pothast, T.Rosenau, G.K.Wurzer, M.Bacher, H.Hettegger, I.Sumerskii, O.Musl, K.Fackler, R.H.Bischof, A.Pothast, T.Rosenau. *Anal. Methods*, **13**, 5502 (2021); <https://doi.org/10.1039/D1AY01241J>
53. J.F.Araneda, I.W.Burton, M.Paleologou, S.D.Riegel, M.C.Leclerc. *Can. J. Chem.*, **100**, 799(2022); <https://dx.doi.org/10.1139/cjc-2022-0041>
54. Y.Tokunaga, T.Nagata, T.Suetomi, S.Oshiro, K.Kondo, M.Katahira, T.Watanabe. *Sci. Rep.*, **9**, 1977 (2019); <https://doi.org/10.1038/s41598-018-38410-9>